processes

MDPI

Review

Catalytic Combustion Hydrogen Sensors for Vehicles: Hydrogen-Sensitive Performance Optimization Strategies and Key Technical Challenges

Biyi Huang [1,2], Yi Wang [3], Chao Wang [3], Lijian Wang [4] and Shubin Yan [1,2,*]

[1] Department of Electrical Engineering, Zhejiang University of Water Resources and Electric Power, Hangzhou 310018, China
[2] Zhejiang-Belarus Joint Laboratory of Intellingent Equipment and System for Water Conservancy and Hydropower Safety Monitoring, Zhejiang University of Water Resources and Electric Power, Hangzhou 310018, China
[3] Taizhou Institute of Measurement Technology, Taizhou 318001, China
[4] Zhejiang Key Laboratory of Digital Precision Measurement Technology Research, Zhejiang Institute of Quality Sciences, Hangzhou 310018, China
* Correspondence: yanshb@zjweu.edu.cn

Abstract

As an efficient and low-carbon renewable energy source, hydrogen plays a strategic role in the global energy transition, particularly in the transportation sector. However, the flammable and explosive nature of hydrogen makes leakage risks in enclosed environments a core challenge for the safe promotion of hydrogen fuel cell vehicles. Catalytic combustion sensors are ideal choices due to their high sensitivity and long lifespan. Nevertheless, they face technical bottlenecks under vehicle operational conditions, such as high-power consumption caused by elevated working temperatures, slow response rates, weak anti-interference capabilities, and catalyst poisoning. This paper systematically reviews the research status of catalytic combustion hydrogen sensors for vehicle applications, summarizes technical difficulties and development strategies from the perspectives of hydrogen-sensitive material design and integration processes, and provides theoretical references and technical guidance for the development of catalytic combustion hydrogen sensors suitable for vehicle use.

Keywords: catalytic combustion hydrogen sensors; sensitivity; technical bottleneck; vehicle operational condition; material design; MEMS

check for updates

Academic Editors: Carmen Branca and Miguel Ladero Galán

Received: 13 June 2025
Revised: 9 July 2025
Accepted: 24 July 2025
Published: 27 July 2025

Citation: Huang, B.; Wang, Y.; Wang, C.; Wang, L.; Yan, S. Catalytic Combustion Hydrogen Sensors for Vehicles: Hydrogen-Sensitive Performance Optimization Strategies and Key Technical Challenges. *Processes* **2025**, *13*, 2384. https://doi.org/10.3390/pr13082384

Copyright: © 2025 by the authors. Licensee MDPI, Basel, Switzerland. This article is an open access article distributed under the terms and conditions of the Creative Commons Attribution (CC BY) license (https://creativecommons.org/licenses/by/4.0/).

1. Introduction

With the rapid development of society, economy, and technology, humanity's demand for energy has been continuously increasing. To fundamentally address the dual crises of energy depletion and environmental pollution, it is urgent to establish an efficient and low-carbon renewable energy system. Hydrogen energy, with its wide sources, high energy density, and clean and pollution-free characteristics, has become a strategic choice for energy transition in many countries. The International Hydrogen Energy Commission predicts that by 2050, hydrogen will account for 18% of the global energy consumption structure, with transportation being an important field for future hydrogen energy applications [1]. Hydrogen fuel cells achieve efficient energy conversion through direct electrochemical transformation, breaking through the limitations of the Carnot cycle, and are significantly superior to internal combustion engines in terms of energy efficiency and

environmental friendliness [2]; its characteristics of no combustion process, zero emissions, and silent operation have made it a strategic direction for the global automotive industry transformation [3].

Despite the broad prospects of the hydrogen economy, safety remains a major technical issue hindering hydrogen promotion. Hydrogen is the lightest gas known, making it highly prone to escape, and it has a wide flammable range in air (4–75.6%). In recent years, hydrogen explosion accidents have occurred frequently, triggering public concerns about large-scale hydrogen deployment. Hydrogen safety incidents are directly linked to leakage. Compared with massive leaks in open environments, slow and undetectable leakage in enclosed spaces poses a more serious threat of fire and explosion. The interior of hydrogen fuel cell vehicles is structurally complex, with potential leakage points at various pipeline interfaces and reaction chamber drain ports. Although hydrogen diffuses 3.8 times faster than air, it can still accumulate rapidly in relatively enclosed environments under natural ventilation, necessitating the rational arrangement of ventilation equipment and sensors [4]. On the positive side, hydrogen's low density offers unique advantages over other fuels. For example, in open areas, the rapid escape of large amounts of leaked hydrogen results in upward jet flames, whereas gasoline leakage adheres to the vehicle's bottom, making it difficult to volatilize and dissipate, thus causing more severe fire accidents. Therefore, automatically detecting hydrogen release through hydrogen detectors, shutting down the battery system, and activating alarms and mechanical ventilation devices can effectively ensure the safety of hydrogen use.

With the deepening of research on the safety of hydrogen handling and utilization, the large-scale implementation of hydrogen fuel cell vehicles will become feasible. The development of hydrogen sensors, as a prerequisite for the promotion of fuel cell vehicles, has long been a focus of the U.S. Department of Energy, which has proposed performance requirements for vehicle hydrogen sensors (Table 1) [5]. There are no clear regulations on the service life yet, but one car manufacturer has set a lifespan target of 15 years [5].

Table 1. Technical Performance Requirements for Hydrogen Sensors Used in Automotive Systems. Reprinted with permission from Ref. [5]. 2009, Professor T. Nejat Veziroglu. Published by Elsevier Ltd.

Parameter	Performance Requirements
Detection Range	0~4%H_2
Response Time (t_{90})	<3 s
Recovery Time (t_{10})	<3 s
Ambient Temperature	−40~125 °C
Ambient Humidity	0~100%RH

According to different detection principles, hydrogen sensors are classified into catalytic, electrochemical, semiconductor, optical fiber, acoustic, thermal conductivity, and mechanical types, and appropriate sensors can be selected according to specific applications. Table 2 lists the characteristics of several mainstream hydrogen sensing technologies (the service life here does not take into account accelerated aging factors such as vehicle vibration and thermal shock) [6]. The internal working environment of hydrogen fuel cell vehicles is relatively harsh, and electrochemical, resistive, optical, and other types all have significant application barriers. Boon-Brett conducted a total of seven different performance tests on 39 commercially available sensors using catalytic, electrochemical, metal oxide semiconductor, and thermal conductivity detection principles. Based on the test results, their applicability as automotive hydrogen safety sensors was evaluated, and it was concluded that catalytic combustion sensors performed the best [7]. As can be seen from Tables 1 and 2, catalytic

combustion sensors have incomparable advantages in sensitivity and service life, making them an ideal choice for onboard hydrogen leakage detection. For example, the hydrogen fuel cell vehicle Mirai launched by Toyota is equipped with the FH2-HY series catalytic combustion hydrogen sensor module from Japan's FIS Corporation, which features linear output, fast response, and long service life, with the sensor power consumption at the milliwatt level [8]. However, over time, the sensor based on this principle can experience many failure modes, which are largely related to the complex vehicle environment. The first is silicon poisoning. In the entire vehicle and fuel cell system, silicone tubes are often chosen for some pipeline connections, and there may also be silicone-containing substances in the sealing materials of the stack. If these components are improperly selected, they may release siloxane substances during use. Siloxane substances will react and polymerize with hydrogen and oxygen on the surface of the detection element, generating attachments such as SiO_2, which blocks the contact between hydrogen and the catalyst, thereby causing the performance of the entire hydrogen concentration sensor to decline. The second is damage from high hydrogen concentration. Hydrogen and oxygen react on the catalyst layer to generate heat, which is used as the basis for detecting hydrogen concentration. However, when the sensor is exposed to an excessively high concentration of hydrogen, a large amount of heat is generated instantaneously, causing the surface temperature of the element to rise sharply, which can lead to the peeling and sintering of the catalyst layer, causing the sensor to fail. Up to now, there are few hydrogen sensors on the market that can simultaneously meet the performance parameters in Table 1. The difficulties lie in the following: the (1) high operating temperature of the catalyst, which brings safety hazards and high operating energy consumption; (2) slow response rate, mainly due to the kinetic limitations of the hydrogen-oxygen reaction; (3) cross-sensitivity, as the detection principle is based on changes in heat during the oxidation reaction, so other reactive substances in the environment will interfere with the sensor measurement results; and (4) short service life, which is caused by catalyst sintering and agglomeration as well as pollutant poisoning leading to failure.

Table 2. Comparison of Various Sensing Technologies. Reprinted with permission from Ref. [6]. 2021, Elsevier B.V.

Sensing Technologies	Lifestime (Year)	Response Time (s)	Power Consumption (mW)	Defect
Thermal conductivity	>5	<15	<500	High power consumption; cross-interference from other gases (e.g., He); low precision; high detection limit; susceptible to temperature influence.
Electrochemical	~2	<30	2~700	High cost; short service life; cross-sensitivity; requirement for special electrolytes; need for regular calibration; poor low-temperature performance; catalyst poisoning and aging; sensitivity to temperature changes.
Metal Oxide	2~4	<30	<800	High power consumption; low precision; cross-sensitivity to other gases and humidity; poor selectivity; requirement for O_2 participation; memory effect; long non-linear response time.
Optical	<2	<60	~1000	Short service life; cross-sensitivity; sensitivity to ambient light interference and temperature changes; high cost.

Table 2. *Cont.*

Sensing Technologies	Lifestime (Year)	Response Time (s)	Power Consumption (mW)	Defect
Catalytic combustion	>5	<20	~1000	High power consumption; cross-interference from combustible gases; high detection limit; requirement for O_2 participation; need for regular calibration.

To address the above issues, solutions can be approached from two aspects: enhancing the reactivity, selectivity, and stability of hydrogen-sensitive materials and optimizing device structures. In recent years, advancements in Micro-Electro-Mechanical Systems (MEMSs) technology have reduced power consumption through device miniaturization [9]. However, high-performance catalytic sensors based on MEMS are rarely industrially produced due to complex preparation processes and high costs. In summary, although catalytic combustion hydrogen sensors show promising prospects for vehicle-mounted hydrogen sensing, their power consumption and reliability are still insufficient to meet market demands, making the research on high-performance hydrogen sensors extremely urgent. Therefore, this paper focuses on the performance optimization of vehicle-mounted catalytic combustion hydrogen sensors, reviews the strategies from two aspects of catalyst design and integration process, discusses the methods to optimize sensor response performance, reduce power consumption, and improve selectivity and stability, so as to provide references for the development of catalytic combustion hydrogen sensors suitable for vehicle-mounted applications.

2. Working Principle of Catalytic Combustion Hydrogen Sensors

When the environment contains no catalyst or ignition source, hydrogen undergoes spontaneous oxidation at temperatures above its ignition point (585 °C). However, in the presence of catalytic metals such as Pd, Pt, and Ru, the temperature of the hydrogen oxidation reaction can be significantly reduced [10,11]. Platinum wire exhibits a linear resistance-temperature characteristic, making it commonly used in fabricating thermistors and hydrogen-sensitive elements. The heat generated by the sensitive element is proportional to the volume fraction of hydrogen: the greater the temperature increase in the platinum wire, the more significant the increase in its resistance value. As shown in Figure 1, a traditional catalytic combustion sensor comprises two ceramic bead elements based on electrically heated platinum wire coils: a sensitive element and a compensation element, which are connected to the required measurement circuit via pins.

A Wheatstone bridge is formed by the sensitive element (R_D), compensation element (R_C), and two fixed resistors (R_1 and R_2). At a constant operating temperature, when no detected gas is present, the bridge is in equilibrium, i.e., $R_C \cdot R_2 = R_D \cdot R_1$, and the output $U_{OUT} = 0$. When hydrogen is present, the flameless combustion of hydrogen causes the temperature of the sensitive element to rise, altering its resistance. The compensation element, without undergoing the reaction, maintains its resistance, thus breaking the bridge balance and outputting a stable voltage signal U_{OUT} proportional to the gas concentration [12]. If the resistance variation in the sensitive element is ΔR_D, the output voltage signal is expressed as Equation (1), as follows:

$$U_{OUT} = V_+ \times \Delta R_D / (\Delta R_D + R_D + R_C) \quad (1)$$

where U_{OUT} is the output voltage, V_+ is the supply voltage, R_D is the resistance of the detection element, and ΔR_D is the resistance variation. The ΔR_D can be described by Equation (2), as follows:

$$\Delta R_D = \alpha \cdot \Delta T = \alpha \cdot Q/c = \alpha \cdot n \cdot \Delta H/c \quad (2)$$

where α is a constant, the temperature coefficient of the platinum electrode, ΔT, is the temperature change in the electrode before and after contacting the target gas, Q is the heat generated by catalytic combustion on the electrode, c is the heat capacity of the electrode, n is the concentration of the target gas, and ΔH is the heat of catalytic combustion. Therefore, the hydrogen concentration can be measured based on the output voltage signal U_{OUT}.

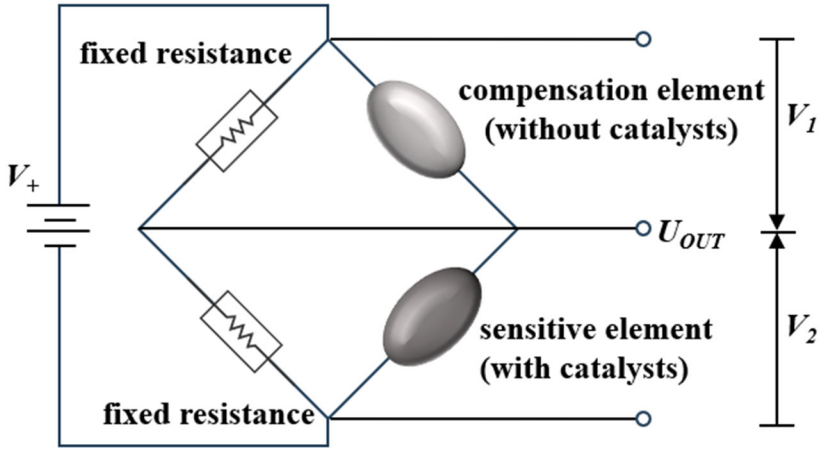


Figure 1. Schematic diagram of catalytic combustion hydrogen sensing detection.

3. Optimization of Hydrogen-Sensitive Materials

Under normal conditions, the temperature required for the reaction between H_2 and O_2 is above 500 °C, but the activation energy of the hydrogen-oxygen recombination reaction is reduced in the presence of a catalyst [11]. Pt is often used as a catalytic material, and the oxidation of H_2 on Pt can be explained by the traditional Langmuir–Hinshelwood (L–H) mechanism, that is, when O_2 and H_2 come into gas/solid contact with Pt sites, they are dissociated into active O and active H, and the generated H_2O is desorbed from the surface in the form of gas. In essence, hydrogen-sensitive materials are hydrogen oxidation catalysts. To enhance hydrogen detection, it is necessary to optimize the reaction pathway of hydrogen oxidation to improve the reaction rate and toxicity resistance. The catalytic effect is mainly determined by the electronic properties of the catalyst. Therefore, understanding the behavior of H_2, O_2, and pollutants on the catalyst surface, precisely regulating the electronic and chemical environment of the catalyst, and designing low-temperature and efficient hydrogen oxidation catalysts are crucial for the development of high-performance hydrogen sensors.

3.1. Design Methods for High-Performance Hydrogen Oxidation Catalysts

3.1.1. Reaction Mechanism

Pt and Pd are used in hydrogen sensors due to their excellent hydrogen dissociation and adsorption properties [13–15]. For Pt, the elementary steps of H_2 oxidation are as follows [16,17]:

$$H_{2,gas} + 2^* \leftrightarrow 2H_{ads} \quad (3)$$

$$O_{2,gas} + 2^* \rightarrow 2O_{ads} \quad (4)$$

$$O_{ads} + H_{ads} \leftrightarrow OH_{ads} + ^* \quad (5)$$

$$OH_{ads} + H_{ads} \rightarrow H_2O_{gas} + 2^* \quad (6)$$

$$OH_{ads} + OH_{ads} \rightarrow H_2O_{gas} + O_{ads} + * \quad (7)$$

where * is a vacant adsorption site. In a kinetically controlled system, step (1) is close to equilibrium, and steps (3–5) are fast reactions. The reaction rate is mainly limited by the adsorption and activation of O_2 on the hydrogen-covered surface (Equation (4)). Especially at low temperatures, the reaction is under kinetic control, and the dissociative adsorption step of O_2 becomes slower. Schwarzer et al. investigated the mechanism of the hydrogen oxidation reaction on Pd catalysts. The elementary reactions are similar to those on Pt, and they suggested that the hydrogen oxidation reaction has a complex relationship with the oxygen coverage and the density of step sites (Figure 2) [18]. The author's research through DFT and transition state theory reveals that there is a synergistic effect among the three stable states of oxygen atoms at the step sites. Two oxygen atoms can induce the third oxygen atom to bond nearby, resulting in a significantly higher reactivity than that of individual oxygen atoms, thereby influencing the rate-determining step of the reaction. The synergistic interaction resulting from the increase in oxygen atom coverage corresponds to the formation of a "zigzag" oxygen atom modified structure on the Pd step surface, and this situation results in a significant reduction in the energy barrier for the formation of OH* at the $O^*_{down\text{-}step}$ site (RPBE: 0.64 eV, PBE: 0.60 eV), which is lower than the energy barrier at the $O^*_{up\text{-}step}$ site (RPBE: 0.93 eV, PBE: 0.93 eV). Therefore, on the oxygen-rich surface, through the cooperative effect between the oxygen atoms bound to the Pd step sites, the energy barrier of the OH conversion reaction is reduced, and the OH dissociation into the reaction's rate-determining step occurs. In general, by enhancing oxygen supply and reducing the activation energy barrier of O_2, the catalytic oxidation activity of H_2 can be improved, and the response rate and sensitivity of the sensor can be enhanced.

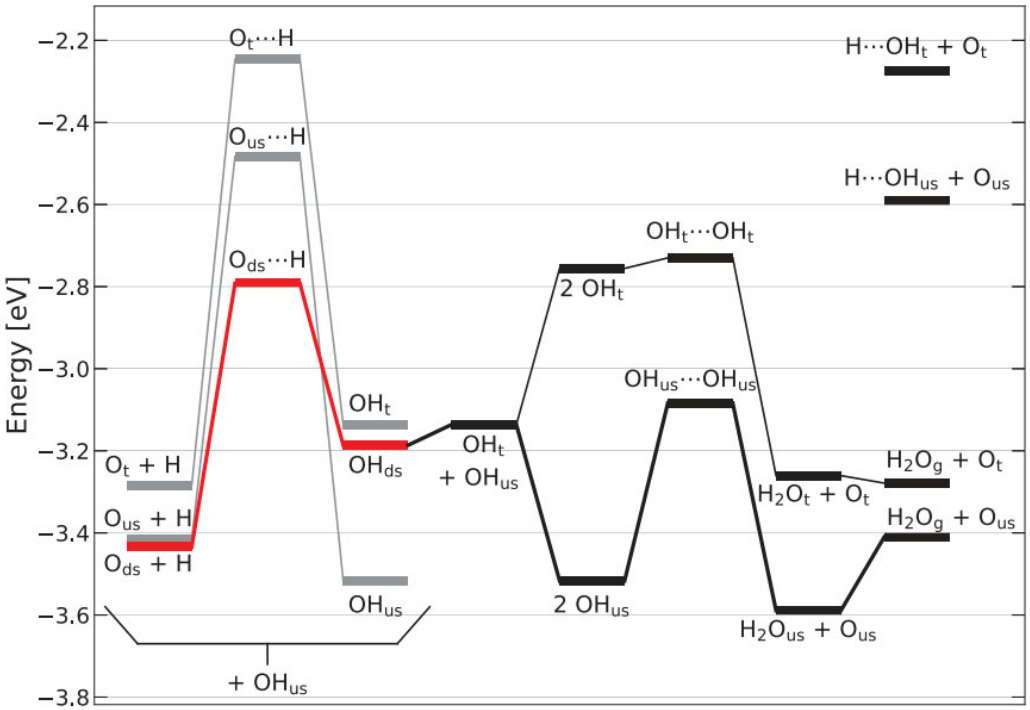


Figure 2. The dominant reaction flux on Pd(332) at elevated O coverages (red) involves OH formation at the O downstep site, diffusion of OH to terraces, and subsequent trapping at steps, followed by disproportionation to form water. At low O* coverages, OH is formed at the $O_{up\text{-}step}$ site. The energy

of an additional OH_{upstep} adsorbate molecule has been added to all energies along the OH formation pathway to ensure mass balance in the subsequent disproportionation reaction. Reprinted with permission from Ref. [18]. 2024, The American Association for the Advancement of Science.

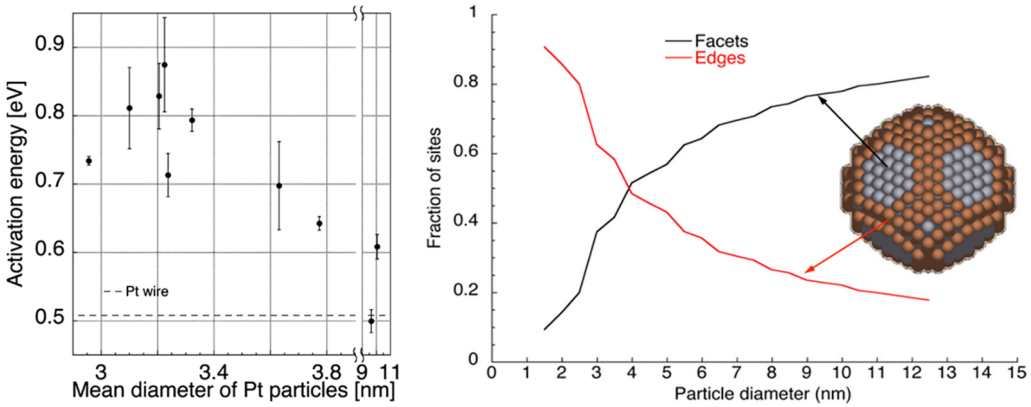
However, the special absorption of Pd for H leads to the fact that the control mechanism and kinetics of the intermediate reaction stage remain elusive under different gas conditions. This is due to the interaction of the catalyst's adsorption, atomic diffusion, and synchronous phase transformation. Liu et al. studied the dynamic behavior of water generation related to the formation of reversible hydrogenated palladium and captured the reaction images in real time with nanoscale spatial resolution [19]. It was found that when H_2 was pre-adsorbed, the H atoms could easily adsorb onto the Pd surface and rapidly diffuse into the lattice. Subsequently, when O_2 was introduced, a hydrogen oxidation reaction was triggered. The internal H atoms could continuously diffuse to the surface to participate in the reaction, and the reaction barrier was relatively low. When both H_2 and O_2 were present, H would compete with O atoms for the active sites on the Pd surface, resulting in a limited reaction rate. However, when O atoms were pre-adsorbed, the O atoms had a strong affinity for the octahedral sites on the Pd surface ($\Delta E = -0.47$ eV), causing the Pd surface to be saturated with O atoms. This led to significant changes in the hydrogen adsorption and diffusion pathways on the Pd surface, hindering the hydrogen adsorption process and inhibiting the reaction from proceeding. Based on the above analysis, both excessively high or low coverage of O_2 is not conducive to the occurrence of the hydrogen oxidation reaction. Developing a catalyst with dual adsorption activation sites for H_2 and O_2 is one of the feasible methods to improve the reaction activity.

3.1.2. Enhancement of the Intrinsic Activity of Catalyst

While extensive research has been conducted on the industrial catalytic combustion of hydrogen, studies on catalytic combustion-type hydrogen-sensitive materials remain relatively scarce. Both processes are based on the hydrogen oxidation reaction. In investigations of hydrogen catalytic oxidation, Wettergren et al. [16] discovered through experiments and theoretical calculations that the apparent activation energy of hydrogen oxidation on Pt particles strongly depends on particle size. The activation energy barrier generally increases with larger particle sizes, approaching that of Pt wires (Figure 3). This phenomenon is hypothesized to arise from the increased number of undercoordinated sites (e.g., edges and corners) as Pt particle size decreases, enhancing the sticking coefficient of O_2 and thereby accelerating its contribution to the reaction. This research highlights the impact of competitive adsorption and activation between H_2 and O_2 on the reaction kinetics, yet the dependence of the oxygen sticking coefficient on hydrogen coverage remains to be explicitly determined.

Singh et al. [20] experimentally found that Pd and Pt are highly active for hydrogen dissociative adsorption, and Pd (~200 K) has a lower temperature for O_2 dissociation compared to Pt (~400 K). Therefore, benefiting from the excellent hydrogen and oxygen dissociation properties of Pd, the activation energy for hydrogen oxidation over PdCZ (CZ represents the Co_3O_4–ZrO_2 composite support) is two times lower than that over PtCZ. Kim et al. [21] prepared a Pd-Cu/Al_2O_3 composite catalyst using Pd and Cu, which promoted the dissociative adsorption of H_2 and O_2, achieving efficient hydrogen oxidation at low temperatures. From this perspective, adding catalyst components with high-efficiency oxygen adsorption and activation capabilities can enhance the oxidation reaction rate. According to reports in the literature, oxygen activation sites mainly include ultramicropores, carbon defects, nitrogen-doped atoms, and active metals. Compared with industrial hydrogen catalytic combustion reactions, hydrogen sensors operate at lower temperatures, expanding the selection range of catalytic materials, such as the use of carbon materials. Among

them, graphene has enormous advantages in the field of gas-sensitive sensing due to its high specific surface area and strong adsorption of certain molecules [22]. Studies have found that the ultramicropores (~0.4 nm) formed by the close arrangement of graphene layers impose spatial constraints [23]. Due to the overlap of adsorption potentials on the graphene walls, the adsorbed molecular oxygen experiences distortion of the O=O bond. Meanwhile, the sp^2-conjugated graphene walls transfer their π^* electrons to the adsorbed molecular oxygen, thereby promoting the formation of superoxide radicals and accelerating the oxidation reaction. In addition, Long et al. discovered that oxygen molecules can be adsorbed and activated at graphitic nitrogen sites, participating in the reaction by forming sp^2-hybridized intermediate products N-O_2 [24]. It is worth noting that the adsorption of water molecules on the catalyst can block active sites, while the hydrophobicity of graphene can inhibit the impact of high humidity on sensor performance [25]. Graphene materials have been successfully used to develop low-power catalytic combustion-type hydrogen sensors, achieving a response speed of <1 s [26]. However, the integration of graphene with MEMS technology still faces two core challenges: the large-scale scalability of the synthesis process and the environmental adaptability of graphene-based sensors [22]. Future research should focus on three key technological breakthroughs: enhancing the repeatability of graphene properties in large-scale production; strengthening the long-term stability of sensors in complex environments; and developing low-cost and high-yield manufacturing technologies to promote the commercialization process of graphene MEMS gas sensors. Furthermore, carbon-based materials such as carbon nanotubes [27] and carbon nitride materials [28] also possess the advantage of enhancing gas sensing performance. However, their poor stability and repeatability remain significant issues that need to be addressed urgently.



(**a**) (**b**)

Figure 3. (**a**) Size-dependent apparent activation energy of hydrogen oxidation on Pt nanoparticles; (**b**) Fraction of surface and edge sites as a function of Pt nanoparticle size (diameter). Reprinted with permission from Ref. [16]. 2015, American Chemical Society.

Reducible supports (such as CeO_2, TiO_2, SnO_2, etc.) possess catalytic oxidation activity due to their abundant oxygen vacancies and high oxygen storage capacity (OSC) and are widely applied in the oxidation of combustible gases [29]. Although inactive supports (such as ZrO_2, etc.) lack reasonable OSC, they exhibit high thermal stability. The performance of supports can be improved by coupling different supports to prepare multicomponent supports. Singh et al. [20] doped Pt or Pd in the form of ions into the CeO_2/ZrO_2 binary support and found that the reaction only occurs on Pt or Pd at low temperatures, following the L–H mechanism; when the temperature > 100 °C, the oxygen storage capacity of the support comes into play, following the MvK (Mars-van Krevelen) mechanism (Figure 4).

The MvK mechanism is essentially different from the traditional L–H. Lattice oxygen in the catalyst directly participates in the oxidation of the reactants, while gaseous oxygen molecules are responsible for reoxidizing the reduced catalyst. This temperature-dependent reaction mechanism is common in reducible supports [30,31]. To promote low-temperature reactions, the availability of lattice oxygen (enhancing oxygen migration ability) can also be improved through the design of crystal structures, thereby accelerating the low-temperature reaction rate [32].

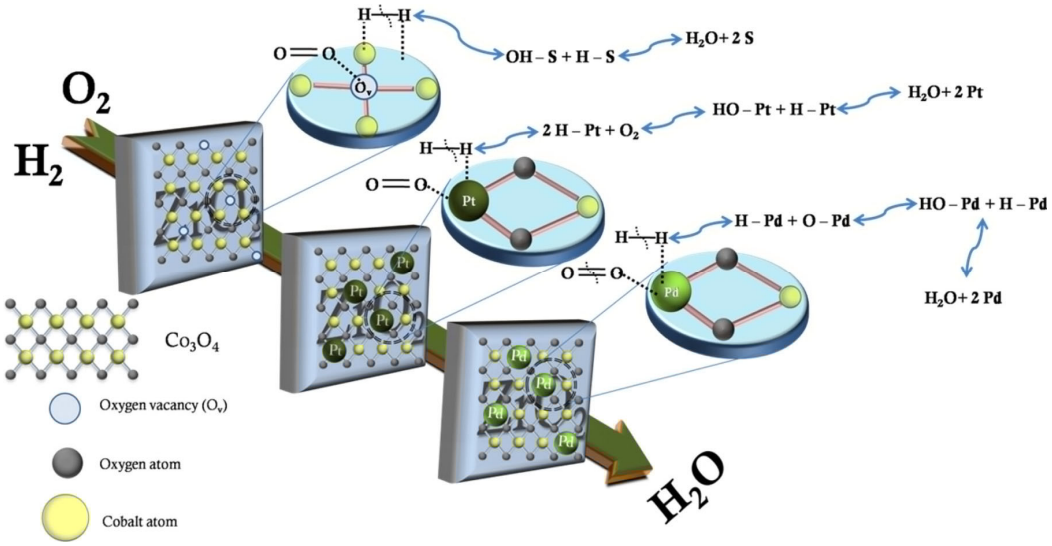
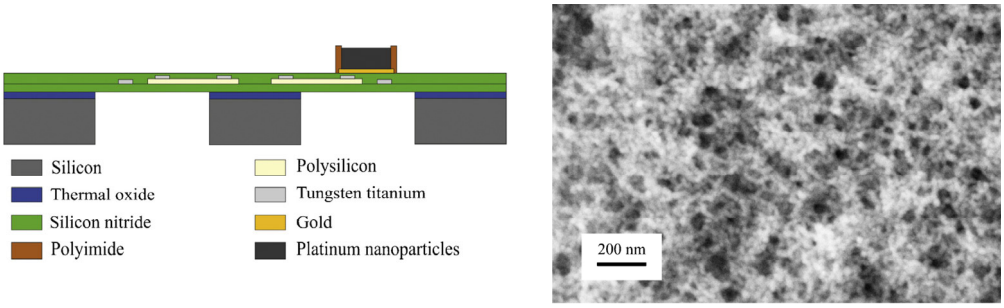


Figure 4. Mechanisms of hydrogen catalytic oxidation over CeO_2/ZrO_2, $Pt/CeO_2/ZrO_2$, and $Pd/CeO_2/ZrO_2$ [20].

3.1.3. Improvement in Catalyst Stability

Noble metal nanoparticles are relatively dispersed and small in size but they are prone to sintering and agglomeration during use, leading to a decline in sensor performance. Therefore, active components usually need to be fixed on supports, and commonly used supports include carbon materials and metal oxides. Han et al. [33] studied Pd/TiO_2 and Pt/TiO_2 nanotube catalysts and found that compared with traditional pure Pd and pure Pt catalysts, the sensors showed higher responses. This result is not only due to the uniform dispersion of Pd and Pt particles at the nanoscale on TiO_2 nanotubes but also because of the good adsorption properties of hydrogen on the surface of TiO_2 nanotubes, which promotes the catalytic oxidation of hydrogen on Pd and Pt. However, supports often have relatively large heat capacities, which increases system heat loss [34,35]. Researchers have proposed using surfactants to stabilize nanoparticles as an alternative solution, which can reduce the heat capacity of the catalyst and thus lower power consumption [35,36]. The main function of surfactant ligands is to form a space between two nanoparticles to prevent agglomeration and sintering. Brauns et al. [35] employed the bifunctional ligand phenylenediamine (PDA) to stabilize platinum (Pt) nanoparticles, creating a highly porous "ligand-linked" nanoparticle network that facilitates gas diffusion (Figure 5a). This design builds upon monodentate ligand systems to achieve enhanced operational stability. The PDA molecule, featuring dual amine head groups, acts as a crosslinking agent to bind two distinct nanoparticles, thereby constructing a mechanically rigid three-dimensional network (Figure 5b). In addition, the PDA ligand also acts as a spacer, which can prevent the sintering of Pt particles and result in a high total metal content in the material (73 wt.%). The resulting nanocomposite demonstrates exceptional sensor performance, exhibiting 90% signal response with a <150 ms recovery time when operated at ~100 °C.



(**a**) (**b**)

Figure 5. (**a**) Schematic cross section of the catalytic gas sensor; (**b**) SEM picture of PDA stabilized platinum nanoparticles, illustrating the high porosity and surface, reprinted with permission from Ref. [35]. 2013, Elsevier B.V.

However, the heat resistance of surfactants still faces challenges for long-term stable operation [35]. Graphene has high thermal conductivity [37], which can effectively transfer heat to micro-heaters, and it is thermally stable at high temperatures [38], making it a suitable support material. Moreover, the surface of graphene is rich in functional groups and defects, which can fix catalytic active components highly dispersedly on its surface or interlayers through van der Waals forces or electrostatic interactions. Harley-Trochimczyk et al. used Pt and graphene to prepare a hydrogen sensor based on a micro-hotplate, achieving an excellent stability and response rate [26].

In addition, the deactivation of catalysts such as Pt and Pd is also one of the causes of sensor performance degradation. Studies have shown that the oxidation state of Pt or Pd increases with the progress of the reaction, leading to a decrease in activity [21]. Yazawa et al. found that doping Pt with promoters with higher electronegativity can inhibit the formation of Pt oxides [39]. Therefore, rationally regulating the electrophilic/electrophobic properties of support materials and promoters is an effective means to design active noble metal catalysts in oxidizing atmospheres.

3.1.4. Improvement in Catalyst Mass Transfer Performance

The adsorption of target molecules on the catalyst surface is the first step in heterogeneous catalytic reactions, which largely determines the reaction rate. For catalysts, the key to optimizing adsorption lies in increasing the number of active sites and improving surface properties. The number of active sites is related to the specific surface area of the material. Catalysts with porous microstructures have larger specific surface areas and facilitate mass transfer, thus bringing higher sensitivity and response rates. Meanwhile, the high specific surface area can reduce the usage of catalysts, shrink the size of sensitive regions, and lower costs and energy consumption. Orbe et al. prepared Pt hollow micro-rod structures using ZnO micro-rods as templates via a two-step local hydrothermal method on a SiO_2/TiO_2 substrate [13]. The highly in situ integration enables the sensor to operate at milliwatt-level power, achieving a response speed of 12 s and sensitivity. The research group also prepared cauliflower-like nanostructured Pt crystals in situ on micro-heaters by electrodeposition. Benefiting from abundant active sites and efficient mass transfer performance, the sensor consumes only 8 mW, with a response time shortened to 1.8 s, and can detect H_2 as low as 75 ppm (Figure 6) [40]. In addition, ordered mesoporous structures [14], hollow sphere structures [41], nanotube structures [33], etc., have been widely reported to improve the gas-sensing performance of materials. It should be noted, however, that the preparation of catalysts with complex pore structures strictly depends on preparation conditions and involves complex processes, increasing the production cycle and difficulty of devices.

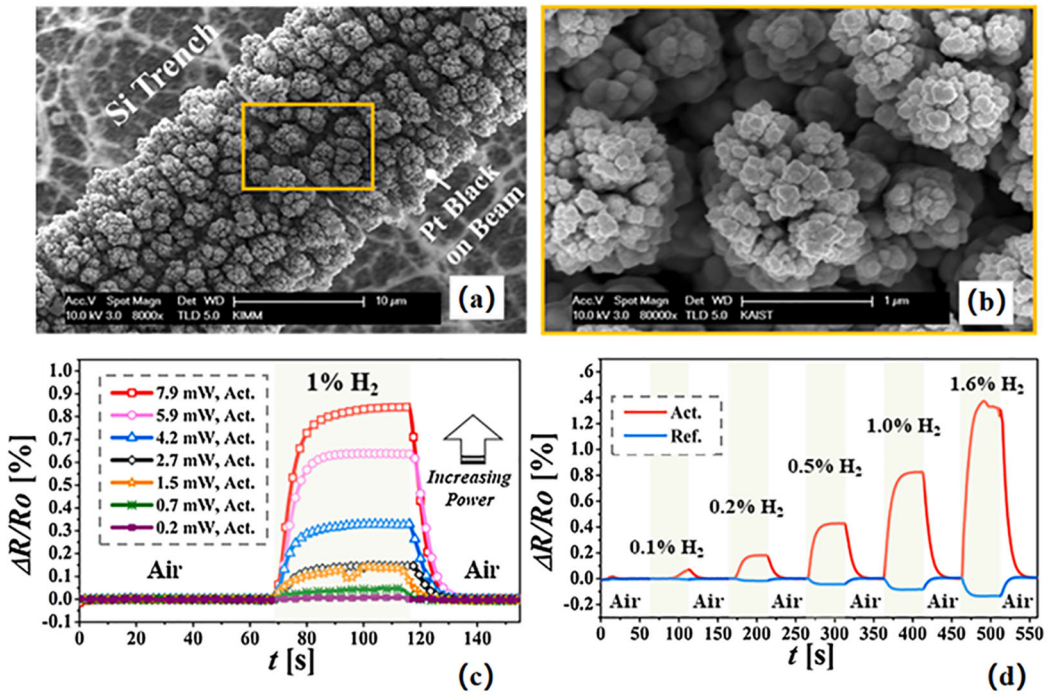


Figure 6. (**a**) FE–SEM image of the active device, showing the pseudo–porous Pt nanostructures synthesized on the suspended microheater, scale bar: 10 μm, (**b**) Magnified FE–SEM image of the highlighted region in (**a**), scale bar: 1 μm, (**c**) Resistance changes in the active devices to increasing power levels, (**d**) Response of active and reference devices to different H_2 concentrations with 8 mW. Reprinted with permission from Ref. [40]. 2020, Elsevier B.V.

Table 3 compares the literature data of the catalytic combustion-type hydrogen sensor mentioned in the previous text. In summary, the competitive adsorption of hydrogen and oxygen on single active sites leads to activity degradation. Therefore, designing different active sites to enhance oxygen supply during the reaction represents a key improvement direction for catalysts. However, the long-term stability of noble metals remains to be addressed. Additionally, the extensive use of noble metals and complex technological processes inevitably increases costs. The design of low-noble-metal or non-noble-metal materials and the development of simple preparation processes are of significant economic benefit for the popularization and application of hydrogen sensors.

Table 3. Comparison of the performance of catalytic combustion-type hydrogen sensors as reported in the literature.

Sensor Structure	Catalyst	Active Area Size	Power Consumption in the Constant Potential Mode (mW)	Response Time	Sensitivity	Stability	Reference
The micro-heating platform based on anodized aluminum	Local Joule heating decomposition for the preparation of 3Pd-Pt	150 μm × 150 μm	116	0.4 s	76 mV/vol.% H_2	<4% response deviation after 14 days of operation	[14]
Floating micro-heat platform	Electrodeposited microrod-like Pt nanostructures	9 μm × 110 μm	4	<12 s	ΔR/R0~0.46% per percent of H_2	Not mentioned	[13]
Floating micro-heat platform	Electrodeposited cauliflower-like Pt nanostructures	9 μm × 110 μm	8	1.8 s	ΔR/R0~0.75% per percent of H_2	Not mentioned	[40]
Floating micro-heat platform	5 wt% Pt/γ-Al_2O_3	200 μm × 200 μm	55.68	0.36 s	~37 mV/vol.% H_2	No response drift after 248 days of operation	[15]

Table 3. *Cont.*

Sensor Structure	Catalyst	Active Area Size	Power Consumption in the Constant Potential Mode (mW)	Response Time	Sensitivity	Stability	Reference
Microheat platform	Pt nanoparticl-loaded graphene aerogel	10 μm × 100 μm	11	0.97 s	ΔR/R0~1.5% per percent of H_2	Not mentioned	[26]
micro-heating platform, fabricated on an alumina plate through a printing process	Pd and Pt/titanate nanotubes	1720 μm × 2000 μm	Not mentioned	<20 s	~77.5 mV/vol.% H_2	Not mentioned	[33]
Micro-heating platform based on Al_2O_3	2%Pt-HZSM5	3000 μm × 1500 μm	Not mentioned	Not mentioned	~18 mV/vol.% H_2	Not mentioned	[42]
Microheat platform	para-phenylendiamine-linked platinum nanoparticles	2000 μm × 2800 μm	30	0.15 s	~220 mV/vol.% H_2	Remain inactive for a week under a pressure of 10,000 ppm H_2	[35]
Microheat platform	Preparation of SnO_2 porous nanomembrane by CVD method	60 μm × 100 μm	35	0.65 s	75.4 mV/vol.% H_2	Maintain a stability of 95% within 200 days	[43]

3.2. Feasible Methods to Improve Hydrogen Selectivity

Currently, commercially available hydrogen sensors operate at relatively high temperatures (300–500 °C), leading to responses to various combustible gases. Studies have confirmed that reducing the sensor temperature can improve hydrogen selectivity due to the low initial reaction temperature of hydrogen (Figure 7) [44,45]. By selecting appropriate catalysts, the sensor temperature can be as low as room temperature [45]. However, because the ambient temperature of hydrogen fuel cell vehicles varies significantly, to avoid detection errors, the sensor operating temperature must be considered. Meanwhile, temperatures above 100 °C can prevent water vapor from condensing on the sensing probe, which may affect detection results.

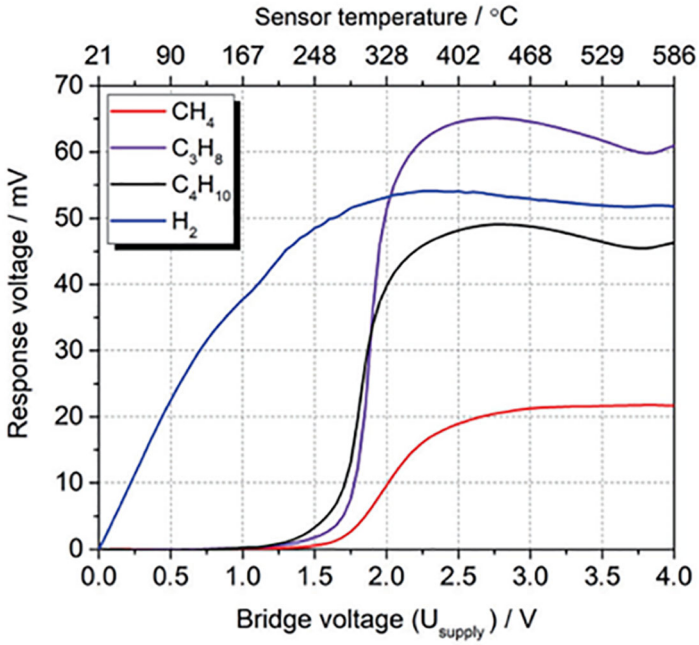


Figure 7. Responses of sensors for hydrogen and hydrocarbons to applied voltage [45].

However, the influence of CO on the hydrogen response at low temperatures remains difficult to resolve. For example, Wang et al. used Pt supported on HZSM5 zeolite as

a hydrogen-sensitive material, which can detect low-concentration H_2 at 150 °C, but unfortunately fails to exclude the effect of CO [42]. It is well-known that noble metals form strong feedback π-bonds with CO due to their unique outer electron structures, leading to strong adsorption, competitive oxidation with H_2, and even catalyst poisoning from excessive CO adsorption. Therefore, improving the low-temperature CO resistance of catalysts presents a more pressing challenge.

Modifying the electronic structure of Pt to weaken its strong adsorption of CO and prevent poisoning has become a consensus in catalyst modification. The energy and occupancy of d-band electrons are two key factors in d-band theory. Chen et al. found that an increase in the energy of the Pt 5d band shows a good correlation with the difference in adsorption energy (ΔE_{ads}) between CO and H_2 [46]. ΔE_{ads} decreases as the energy of the Pt 5d band increases, indicating more intense competitive adsorption between H_2 and CO. Introducing electron-withdrawing groups and defects on the support can reduce the electron occupancy of Pt 5d states, thereby weakening CO adsorption. Designing multi-component catalysts and constructing heterojunctions are believed to enable the regulation of catalysts' adsorption of CO and H_2 through interface electronic control and cooperative catalytic effects [47]. Materials with excellent hydrogen dissociative adsorption activity, such as Pd metal, can be used as additives to improve catalyst selectivity for H_2. Yue et al. [48] found that Pd species in the catalyst exist in the forms of Pd^0, Pd^{2+}, and Pd^+. Among these, Pd^{2+} and Pd^+ rapidly adsorb and activate CO, while Pd^0 species readily adsorb H_2 to form PdH_x, inhibiting CO adsorption and activation. Kim et al. also proposed that a high Pd^0 content facilitates H_2 conversion, and Cu, as an electron donor, promotes the chemisorption of H_2 by Pd [21]. A recent report on precisely regulating the oxidation behavior of CO/H_2 on Pd has analyzed the adsorption behavior of CO/H_2 based on different degrees of the chemical and aggregation states of Pd species [49]. The author used $PdCl_2$ and $CuCl_2{\cdot}2H_2O$ as precursors to prepare Pd-Cu/Al_2O_3 catalysts with different Pd contents by the sol-gel method. X-ray absorption spectroscopy (XAS) was employed to further determine that the Pd^{2+} in the catalyst originated from the Pd-Cl and Pd-O coordination structures. As the content of Pd decreases, Pd transforms from clusters to mainly existing in the form of single Pd species, resulting in an increase in the coordination number of Pd-Cl. This leads to an increase in the degree of electron deficiency of Pd atoms, which will regulate the electron interaction between Pd atoms and copper atoms, increase the binding energy of $Pd_{5/2}$, weaken the ability of H_2 adsorption and desorption/extrusion, and strengthen the adsorption and oxidation of CO. In situ Fourier transform infrared spectroscopy indicates that the CO adsorption peak corresponds to the linear adsorption of CO on the Pd^{2+} substance. It is proposed that the Pd^{2+} substance may be the main active site for CO oxidation. Maintaining the reduced state of Pd during the reaction is the key to improving the selectivity of H_2. Therefore, H_2 selectivity can be achieved by enhancing the oxidation resistance of Pd. Additionally, installing a molecular filter layer (such as a core-shell structure) is a feasible approach to improve selectivity [50], but it increases gas mass transfer resistance. However, due to the small molecular size of CO, the molecular filter layer still struggles to exclude its influence [51].

From the above analysis, it is evident that designing low-temperature catalysts represents a simple and effective approach to improving H_2 selectivity of sensors. In practical application scenarios of sensors, the low content of CO may not cause severe detection errors, but the poisoning effect of trace CO on catalysts cannot be ignored. By regulating the electronic properties of catalysts, CO adsorption can be weakened, and its removal from active sites can be promoted. While weakening the adsorption between catalysts and CO, maintaining their stability and catalytic activity in the reaction environment remains a key challenge in this process.

3.3. Research on Si-Poisoning and Regeneration of Catalysts

Catalyst poisoning by contaminants is a primary cause of output signal drift and sensor failure. In hydrogenation and hydrogen storage systems or fuel cell systems, connecting parts, seals, or heat dissipation materials are typically silicon-containing materials, which release siloxane substances during use. These substances react on the surface of detection elements to generate SiO_2 (Figure 8).

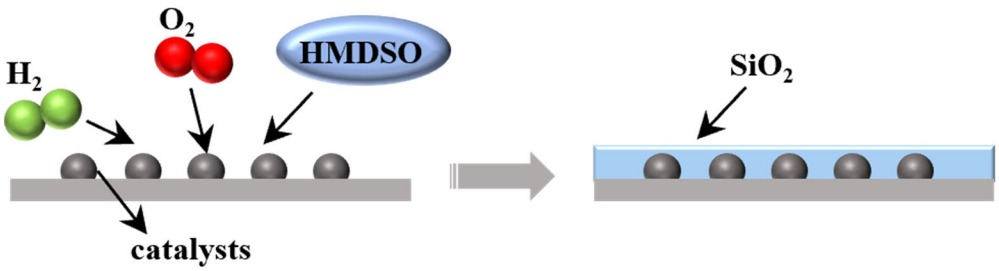


Figure 8. Schematic diagram of silica poisoning of the platinum wire sensitive element.

The poisoning effect of organosilicon compounds on catalysts was first proposed and studied in the 1970s, among which hexamethyldisiloxane (HMDSO) exhibits the most severe toxicity. Initially, HMDSO was considered to have minimal impact on the adsorption of hydrogen and oxygen on Pt [52], but subsequent studies have shown that it can poison Pt sites and reduce the active surface area [53,54]. Matsumiya et al. suggested that the adsorption poisoning effect of HMDS on the catalytic activity of platinum surfaces during hydrogen oxidation reactions is related to the exposure temperature, time, and HMDS concentration [51]. At temperatures below 100 °C and in an atmosphere of 100 ppm HMDS, the catalytic activity maintains the usual level of hydrogen oxidation to a certain extent. However, when the concentration exceeds 500 ppm, even at 100 °C operation, the catalytic activity is strongly inhibited.

Unlike the deactivation mechanism of noble metals, HMDSO deactivates catalysts by reducing the concentration of oxygen vacancies on active supports [55]. Specifically, silicon binds to the surface through oxygen bridges at active sites, forming partial silicon species that cannot dissociate from the catalyst surface. With increased exposure to HDMSO, strong chemisorption as a monolayer and physical multi-layer deposition blocks surface oxygen vacancies and prevents reactants from accessing the catalyst surface. However, SiO_2 is not necessarily the final product: on low-activity materials, HMDSO decomposition products mainly consist of organosilicon and silicates, while on high-activity materials like Pt and Pd, further reactions generate SiO_2 deposition layers [55].

Although research on silicon poisoning resistance of catalytic combustion-type hydrogen-sensitive materials is limited, studies on other gas-sensitive materials indicate that material modification can enhance the silicon poisoning resistance of catalysts. Modification methods mainly include creating physical or chemical barriers [56], surface deposition and modification [55], cladding coverage [57,58], etc. Mohammad et al. [53] found that by leveraging the high affinity of organosilicon for Fe and low mobility for Pt, the development of Pt-doped Fe catalysts can keep more Pt active sites open. However, with increased silicon uptake, multi-layer deposition layers with poor mobility are formed, leading to the permanent blockage of active sites. In the design of cladded catalysts, a double-layer structure of Pd/In_2O_3 sensitive layer combined with the In_2O_3/Al_2O_3 filter layer has been proposed (Figure 9) [59]. Hydrogen, with the smallest molecular size, can easily pass through the filter layer to react in the sensitive layer, while HMDSO is pre-catalytically oxidized into silicon species in the filter layer, improving the sensor's resistance to HMDSO. Based on the fundamental understanding of HMDSO poisoning mechanisms, Kwon et al.

designed an active CeO_2/rGO filter layer, which provides abundant oxygen to the surface, reducing the sensitivity of surface chemical processes to HMDSO [57]. Nevertheless, the above modifications still cannot prevent the complete coverage and deactivation of the catalyst surface by silicon species under long-term poisoning. Therefore, research on catalyst regeneration mechanisms and the design of regeneration procedures is particularly important for extending catalyst service life.

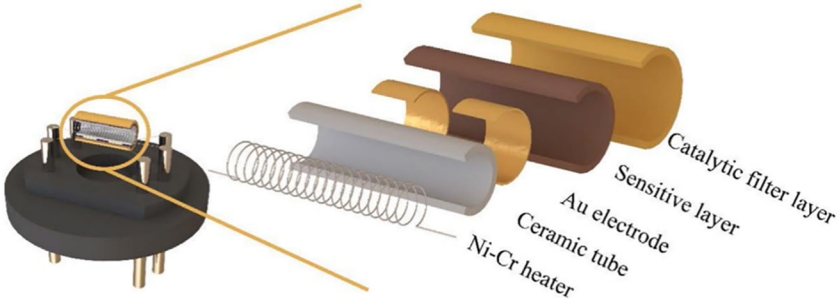


Figure 9. Schematic diagram of the sensor device structure with a double-layer catalytic layer. Reprinted with permission from Ref. [59]. 2022, Hydrogen Energy Publications LLC. Published by Elsevier Ltd.

A thin silicon deposition layer on the catalyst can undergo deep reorganization during heat treatment to re-expose active sites, achieving catalyst regeneration. The catalyst regeneration mechanisms are generally considered to be the following: (i) the silicon deposition layer has migratory properties for redistribution, thereby opening Pt sites, and (ii) silicon species desorb from the surface. Ehrhardt et al. investigated the effect of temperature on the poisoning of HMDS on the Pt surface using XPS analysis methods, and proposed that the interaction between HMDS and Pt occurs through dissociative adsorption [60]. Within the experimental range (700–1100 K), it was observed that Si and O were the main components of the coating layer. It was speculated that this was due to the breakage of the Si-CH_3 bond and the desorption of carbon-hydrocarbon fragments. Below 950 K, poisoned Pt could partially regain activity after heat treatment at 1000 K. The authors believe that at this point, the coating layer did not dissolve from the surface but underwent structural changes in an oxidative atmosphere, eventually forming SiO_2 islands, resulting in some Pt being re-exposed. However, at temperatures above 950 K or after being fully exposed to HMDS, the surface of Pt will be severely contaminated and cannot be regenerated. Arnby et al. subjected Pt/Al_2O_2 and Fe/Pt/Al_2O_2 to 15-h regeneration treatment under room temperature air atmosphere [61]. Through ICP-AES detection, it was found that the Si element on the catalyst did not decrease before and after regeneration. They believed that mechanism (i) was the most reasonable. However, Matsumiya et al. reached a different conclusion [51]. First, they exposed the Pt surface to HMDS at temperatures ranging from 65 to 200 °C and then subjected it to a 2-h thermal treatment in air at 400 °C to re-activate it. Through XPS analysis, it was found that HMDS could rapidly deactivate the catalyst by forming a SiO_2 coating, and after the regeneration treatment, some of the SiO2 on the Pt could be removed.

Additionally, Rasmussen et al. proposed the activation effect of H_2 on poisoned catalysts (Pt/TiO_2) at 500 °C. The reducibility of H_2 leads to the cleavage of Pt-siloxane bonds, and siloxanes desorb as re-volatile compounds or combine with support oxides/hydroxides to release active sites [62]. Different from other parts of the literature, only siloxane species have been reported on the poisoned Pt, while no SiO_2 was found. The author did not provide an explanation for this, perhaps due to differences in the reaction temperature or HMDS concentration. The inconsistency of the HMDS poisoning products has not

been reasonably explained. The formation mechanism of silicon species under different conditions (such as temperature, HMDS concentration, exposure time, etc.) is insufficiently studied (for example, under what circumstances will they be oxidized and decomposed into SiO_2 or silicates, or only adsorbed in the form of siloxanes), which leads to the slow progress of the modification of catalysts for resistance to silicon poisoning. Furthermore, the regeneration procedure design of the poisoned catalyst depends on the study of the regeneration mechanism, and the regeneration mechanism is influenced by the poisoned products. Currently, apart from the regeneration of different poisoned products, there are no research reports yet on the influence of the crystallinity of the generated SiO_2 on the regeneration process, which is a problem worthy of attention. With the development of technology, the introduction of in situ surface spectroscopy technology and in situ imaging technology will help clarify the interaction mode between silicon species and active metal sites under operating conditions and obtain information about the film structure and inhomogeneity. Systematic research on the mechanism of silicon poisoning and the regeneration mechanism will be beneficial for the modification of catalysts against silicon poisoning and the design of active regeneration procedures.

So far, the mechanisms of HMDSO-induced catalyst deactivation and HMDSO dissociation remain unclear, and the surface modification for catalyst deactivation has not been deeply studied. The literature clearly lacks research on H_2 sensors with ultra-fast response and recovery properties against silica poisoning, which limits the market development of such sensors.

4. Device Integration

To achieve a certain reaction rate, sensors typically need to operate at relatively high temperatures. In addition, the inefficient integration of devices also leads to high power consumption. The relatively high power level is a key factor limiting the use of catalytic combustion-type sensors in mobile applications. It is worth noting that high power also poses safety risks. The minimum ignition energy of hydrogen is lower than that of other flammable gases [6], and a weak spark can be dangerous.

The traditional catalytic combustion elements with precious metal wound wires are generally made by winding platinum wires into a spiral shape, then coating them with an alumina precursor solution, sintering them into alumina balls, and finally impregnating them with precious metal catalysts and sintering them. This catalytic combustion element has the problems of low mechanical strength and high power consumption. Manufacturing micro-sensors using micro-electromechanical systems (MEMS) technology is a shortcut to solving the above problems. This sensing element is based on MEMS micro-heaters, which integrate the Pt planar thin-film heating structure on the surface of a silicon substrate. This effectively avoids the risk of circuit interruption in traditional catalytic elements and significantly improves the structural reliability and thermal uniformity of the device. In addition, due to the heated platinum thin film having a thickness of less than 0.1 μm, its electrical resistance is significantly higher than that of wire-wound components (there is an order of magnitude difference in the resistance values between the two). The pronounced resistance-temperature effect enhances sensor sensitivity. The utilization of MEMS-based microheaters as heating elements has become a critical development direction in sensor research, particularly for fabricating low-power catalytic combustion hydrogen sensors.

Despite the development of laboratory-scale catalytic sensors with power consumption below 10 mW, commercial catalytic sensors generally exhibit significantly higher energy consumption. The small dimensions of MEMS devices and the specialized nature of silicon wafer fabrication technologies present substantial challenges in structural design and mass production of high-performance catalytic layers, making these processes both technically

demanding and labor-intensive. Consequently, the realization of a catalytic combustion gas sensor that achieves miniaturization in size, planarization of heating electrodes, rapid catalyst preparation, and scalable manufacturing capabilities would bring transformative benefits to industrial production costs and methodologies in the sensor field.

4.1. Catalytic Layer Integration Method

Catalyst powders are conventionally deposited onto the sensor element surface through traditional integration techniques, including drop-casting, spin-coating, and screen-printing. SiC features high mechanical strength, chemical inertness, and high thermal conductivity. When used as a carrier, it can prevent the formation of hot spots during the reaction process and enhance the safety of the device. Fernandez et al. [63] used SiC monolith foam as the carrier and substrate, then loaded the Pt catalyst onto Al_2O_3 and CeO_2 with high specific surface area, and then coated it in the SiC foam to form a catalyst coating. This catalytic material can start the catalytic combustion of H_2 within a few seconds at a temperature close to room temperature and detect 1% H_2. Li et al. [64] fabricated a catalytic hydrogen sensor by screen-printing Pt heater electrodes onto porous Al_2O_3 substrates and employing wet-impregnation to deposit Pt catalysts onto Al_2O_3 (Figure 10). This configuration demonstrated a relatively high sensitivity (≈30 mV/Vol%) at 245 °C coupled with excellent long-term stability. However, these methods are only applicable to the production of larger-sized sensors due to insufficient fineness. The reduction in the size of MEMS gas sensors makes it difficult to precisely load the sensing material onto the electrode, leading to quality control issues such as poor consistency and unstable contact, which severely limit the advantages of micro-nano devices. The development of precise and controllable on-chip integration technology has become a key challenge, and some emerging fabrication processes based on lithography and patterning have been proposed.

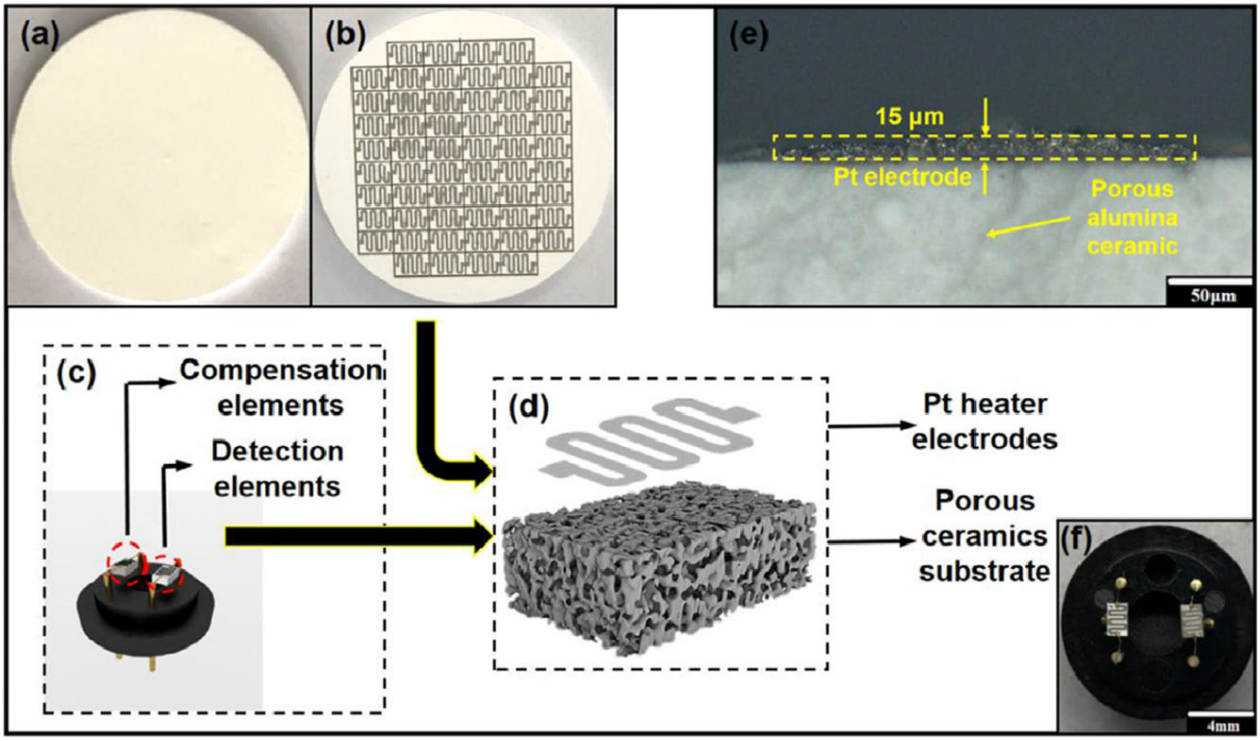


Figure 10. (**a**) Physical drawing of porous Al_2O_3 ceramic sheets; (**b**) Pt heating electrodes mass-produced by screen printing technology; (**c**) Structural diagram of the catalytic combustion sensor; (**d**) Schematic diagram of the preparation of the sensitive element; (**e**) Image of the cross-section of the sensitive element; and (**f**) physical image. Reprinted with permission from Ref. [64]. 2021, Changchun Institute of Applied Chemistry, CAS. Published by Elsevier Ltd.

Given that catalytic combustion gas sensors operate through thermally sensitive mechanisms, efficient thermal coupling between the catalytic layer and substrate is critical for accelerating heat transfer. Direct growth of catalytic materials not only enhances the uniformity of catalytic thin films but also ensures excellent adhesion and thermal contact between the catalyst and substrate. This can be achieved through various in situ fabrication techniques, including hydrothermal processing [13,65], electrodeposition [40], chemical vapor deposition (CVD) [43,66], and magnetron sputtering. Combined with lithography technology, higher integration can be achieved, and the selective deposition of sensing materials in specific areas can also be realized. The typical preparation method of the MEMS gas sensor micro-heater is shown in Figure 11. Kalinlin et al. used porous anodic aluminum oxide (AAO) as the substrate, and through magnetron sputtering, chemical lithography, and ion beam etching technologies, they integrated a Pt heater and a PtPd catalytic layer [14]. Firstly, the aluminum foil is subjected to mechanical and electrochemical polishing, followed by anodic oxidation treatment in 0.3 M $H_2C_2O_4$ solution. After multiple photolithography processes, a patterned Pt heating electrode and substrate structure are successively obtained. Each individual micro-heater is installed in the metal header packages through ceramic support and epoxy adhesive, and a 270-nanometer-thick alumina protective layer is deposited on the surface of the micro-heater using magnetron sputtering. Finally, the author achieved in situ thermal reduction of the catalyst by performing a slight wet impregnation in the active area of the micro-heater. The H_2PtCl_6 and $PdCl_2$ precursors decomposed under the action of Joule heat, directly forming Pd-Pt bimetallic nanoparticles on the surface of the AAO. This in situ calcination process avoids the common sintering method that exposes the entire sensor chip to external high temperatures, preventing damage to the encapsulated part of the microsensor caused by high temperatures and improving its process compatibility with microelectronic devices [67]. Furthermore, the use of electrically heated micro-heaters enables the generation of highly concentrated heat, and this highly integrated preparation method allows for the precise positioning of nanomaterials.

To further reduce heat loss and power consumption, suspended heating platforms have been proposed, which significantly minimize the contact area between heating elements and substrates, enabling effective thermal activation of catalysts at low power levels [40,68]. Orbe et al. [13] developed a ribbon-shaped suspended microheater (9 μm × 110 μm) through multi-step photolithography, employing localized hydrothermal methods to synthesize Pt-based hydrogen-sensitive materials with unique morphologies. The fabrication process involved the following: (1) sputtering SnO_2 seed layers onto the suspended microheater structure; (2) localized hydrothermal synthesis of ZnO microrods by applying precursor solution drops followed by 15-min activation with 50 mW power input across the heater terminals; and (3) secondary localized hydrothermal synthesis of Pt nanomaterials using potassium tetrachloroplatinate as a precursor. Through controlled reduction of Pt on the surface and gradual etching of ZnO, hollow microrod structures with pseudoporous characteristics were ultimately achieved (Figure 12) after optimizing hydrothermal duration, resulting in sensor power consumption as low as 4 mW.

However, while MEMS technology has indeed opened new avenues for developing high-power catalytic combustion hydrogen sensors, these advancements universally involve complex manufacturing workflows-including iterative etching procedures and intricate catalytic layer preparation protocols. Consequently, the development of simplified, gentle in situ fabrication processes for high-performance catalytic layers has become critically urgent. For example, in the case of coplanar structures, since the heaters and comb-shaped finger electrodes are located in the same layer, they can be fabricated in the same deposition step, thereby simplifying the process. The pursuit of such optimized fabri-

cation strategies will directly impact the commercial viability of next-generation hydrogen sensing technologies, enabling broader deployment across energy, industrial safety, and environmental monitoring applications.

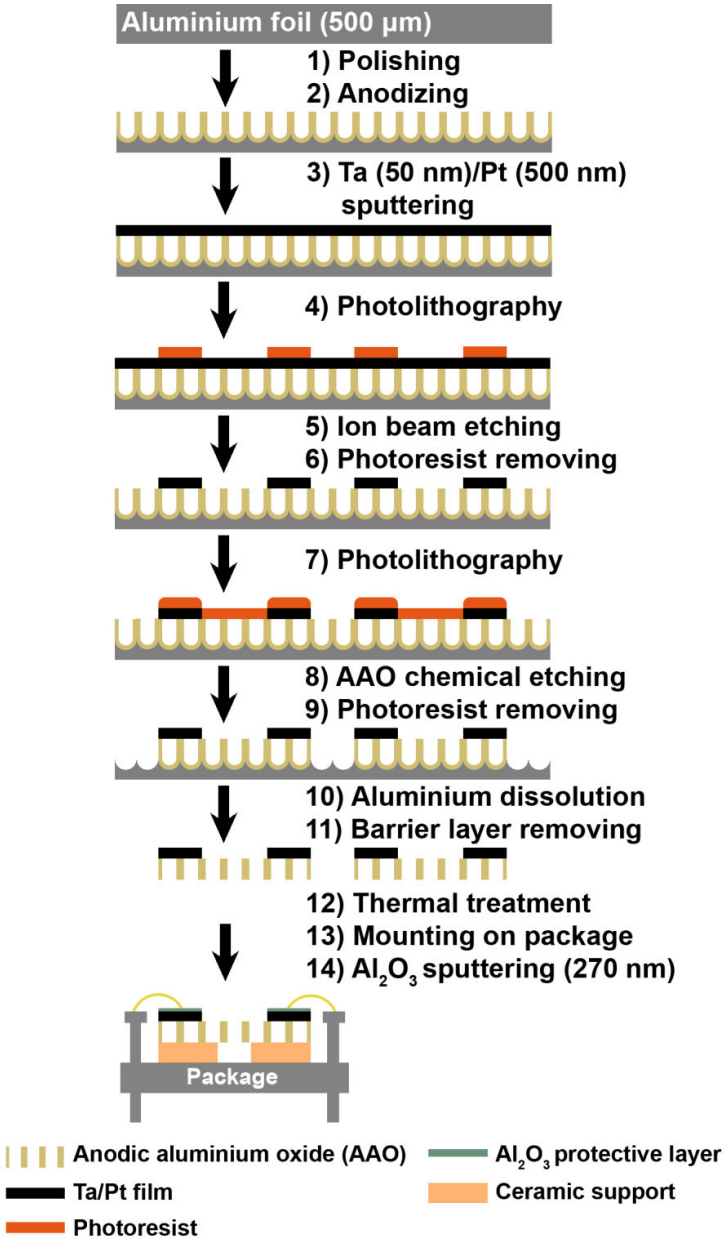


Figure 11. Manufacturing flowchart of a platinum micro-heater. Reprinted with permission from Ref. [14]. 2024, Elsevier.

4.2. Considerations for Device Integration

4.2.1. Weaken the Impact of Environmental Humidity

To enhance the performance of the sensor at low temperatures, the outer shell is usually made of materials that are resistant to cold and have good heat insulation properties, such as polyimide and polyurethane, to reduce heat loss. An internal heating element is integrated, which can preheat the sensing area to the optimal working temperature range at low temperatures, preventing condensation and material brittleness [69]. However, during the operation of hydrogen fuel cell vehicles, the temperature and humidity inside the battery compartment are relatively high. Under such harsh conditions, the output signals of the sensors decrease significantly [70]. At high temperatures, the air humidity is relatively

high, and water vapor will adsorb onto the active sites of the catalyst, thereby inhibiting the hydroxide reaction [71]. To address this issue, methods such as developing hydrophobic catalysts [25], constructing selective water-blocking layers [72], and integrating humidity compensation modules [73] can be employed.

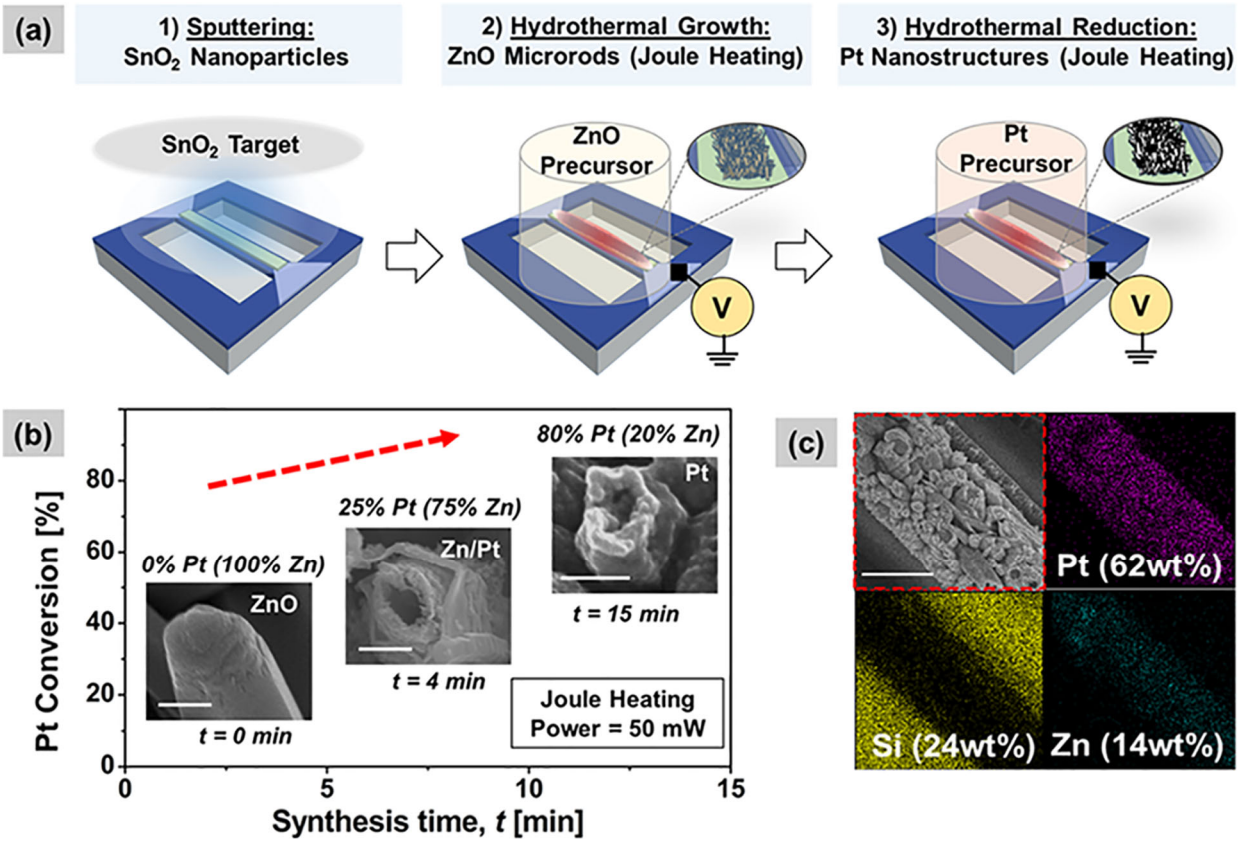


Figure 12. (**a**) Schematic representation of the integration of the Pt nanostructures onto the suspended microheater, based on a sputtering step and two sequential hydrothermal steps; (**b**) Morphological and elemental changes in the ZnO microrods into Pt nanostructures, as a function of synthesis time (in the final hydrothermal process with the Pt precursor), the scale bar is 500 nm; (**c**) EDS mapping of the suspended beam with the integrated Pt nanostructures. The scale bar is 5 μm. Reprinted with permission from Ref. [13]. 2021, American Chemical Society.

4.2.2. Optimization of Mechanical Stability

An additional issue requiring special attention is that, due to the unique usage scenarios of onboard hydrogen sensors (high-speed movement, bumping, etc.), higher requirements are imposed on the mechanical stability of the sensors. For traditional catalytic gas sensors, they are mainly fabricated by coating sensitive materials on a wire-wound Pt coil and then sintering. The three-dimensional structure of the Pt coil in traditional catalytic sensors is extremely sensitive to vibration; that is, there is a problem that the coil is prone to open circuit. With the development of sensors toward integration and miniaturization, integrating the heating structure and sensitive materials to prepare a microthermal platform has the advantages of small size, low power consumption, fast thermal response, and easy integration. The planar electrode structure adopted by the MEMS-based catalytic gas sensor improves the coil vibration problem of the traditional catalytic sensor.

Two key performance parameters of microthermal platforms that receive the most attention are power consumption and temperature uniformity. According to different types of support membrane structures, microthermal platforms can be divided into two categories: continuous membrane type [74,75] and suspended membrane type [76,77]. The

continuous membrane microthermal platform is generally formed by stacking multiple layers, such as heating layers, insulating layers, and sensitive layers, which are processed by backside etching. A typical structural schematic diagram is shown in Figure 13a. It is generally believed that the continuous membrane structure has better mechanical strength, higher reliability at high temperatures, and better temperature uniformity. However, the continuous membrane has fast heat dissipation and large power loss. To reduce power consumption, more researchers prefer to use front-side etching to obtain suspended membrane microthermal platforms. A typical suspended microthermal platform is shown in Figure 13b [77]. The suspended heating platform is connected to the substrate using a cantilever beam structure. Compared with the continuous membrane, the contact area with the substrate is greatly reduced, which reduces thermal conduction loss and enables the catalyst to achieve good thermal activation at low power consumption [13,40,77].

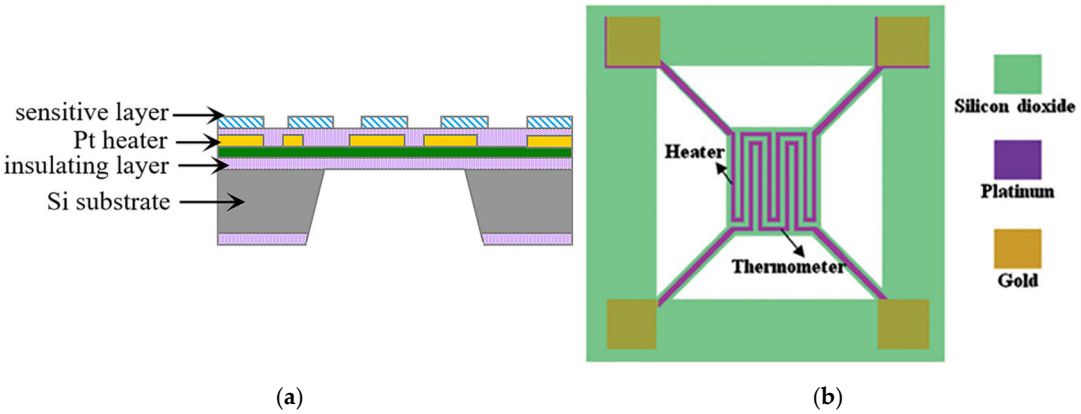


Figure 13. Gas sensor chips based on micro-heating platforms: (**a**) continuous membrane type and (**b**) suspended membrane type, reprinted with permission from Ref. [77]. 2016, The Society for Experimental Mechanics, Inc.

However, the suspended heating platform suffers from attenuation and structural fragility and vulnerability to fracture due to residual stresses during the manufacturing process and thermal mismatch between different layers, especially when the number of support beams is small. This defect may limit its application in vehicle-mounted systems. The appropriate geometric design of the micro-heater and the cantilever is also crucial for achieving further optimized thermal-mechanical performance. With the continuous development of MEMS micro-thermal plate platforms, many optimized classic heater geometric designs have emerged, such as the serpentine structure of the heater [78], double spiral [79], square meander [80], circular meander [81], etc. These designs possess long-term stability and higher manufacturing yield and have always received much attention. Chen et al. fabricated a suspended membrane-type micro-heater chip with a three-layer composite structure, including a Si3N4 support layer, Pt/Ti heater, SiO2 isolation layer, and Au/Cr comb-shaped electrodes [67]. The micro-heater of this chip adopts a circular design, which is conducive to releasing the film stress and loading the sensing material. Xie et al. proposed a hexagonal micro-heater, which integrates six independent sensing channels [82]. At the midpoint of each side, there is a sensing area. The entire hexagonal framework is supported by the beams at the corners, which effectively balances power consumption and mechanical strength. In addition to adjusting the shape of the sensing chip and the structure of the supporting beams, the adoption of a flexible substrate is also an effective way to improve the mechanical stability of the sensor. Xie et al. innovatively proposed a hydrogen sensing chip structure based on an ultra-thin mica substrate [71]. By replacing the brittle silicon-based material with a flexible mica substrate, the sensing chip can maintain a stable

output after being bent over 100 times. Additionally, Pd nanoclusters were magnetron sputtered on both sides of the micro-heating platform as catalysts, effectively increasing the response rate of the sensor (~3 s). Currently, research mainly focuses on the gas sensitivity and power consumption of the sensor, while there is little attention paid to the mechanical stability of the sensor. However, this is an aspect that cannot be ignored in vehicle applications.

The main component of the microthermal platform is the heating wire, whose shape and size design will affect the temperature uniformity, thermal response time, power consumption, mechanical stability, and thermal reliability. In addition to the geometric shape of the heater mentioned above, it is also important to note that high temperature gradients have negative impacts on both the thermal stability of the heating area and the reliability of electromigration. Due to the different thermal expansion coefficients of materials, heating causes different materials to expand at different rates, leading to stress accumulation in the structure, which is finally released through deformation. Liu et al. [83] found that thinner platinum wires fail and break due to electromigration, caused by the inhomogeneity of the internal structure of the thin-film conductor and excessive current density. When the sputtering thickness is increased, the heating wire becomes denser and more reliable, increasing the critical current density, leading to electromigration. However, increasing the thickness of the heating wire also causes a significant increase in power consumption. To promote the development of sensors toward higher reliability, lower power consumption, and intelligence; in the future, multi-dimensional collaborative innovation in terms of materials, structures, and algorithms is still needed. In combination with the strict requirements of the vehicle-mounted scenarios, the commercial and safe application of hydrogen energy vehicles can ultimately be achieved.

4.2.3. Simplification of the Preparation Process

Whether it is a membrane structure or a suspended structure, the layers are arranged vertically in the direction perpendicular to the plane, starting from the bottom and consisting of the substrate, support layer, micro-heater plate, insulating layer, and gas sensor measurement electrode. Due to the fact that the micro-heater plate and the measurement electrode are located on different layers in this vertical structure of the MEMS gas sensor, parasitic electric fields will be generated in the vertical direction, which will cause certain interference to the detection signal of the gas sensor and reduce the performance of the gas sensor [84]. Furthermore, in the manufacturing process of vertical structure MEMS gas sensors, multiple processes such as lithography, sputtering, and Lift-off are required to separately fabricate the measurement electrodes and micro-heatsheets of the MEMS gas sensors. This makes the process relatively complex, which is not conducive to reducing the production cost of the devices and improving the yield of batch product processing. Researchers have proposed a coplanar structure MEMS gas sensor, where the measurement electrodes of the gas sensor and the micro-heatsheet are designed on the same plane, and the insulating layer is used to isolate the heating electrodes of the micro-heatsheet and the measurement electrodes of the gas sensor. The coplanar MEMS gas sensor can effectively reduce the influence of parasitic electric fields in the vertical direction on the sensor performance and simplify the processing flow of the gas sensor [67]. However, the temperature uniformity of the coplanar structure is relatively poor. It needs to be improved through the optimization design of the chip and heating wire geometries, as well as the development of new materials.

4.2.4. Development of Integrated Sensors

Given the wide range of temperature and humidity conditions in vehicle-mounted applications, a study on commercial off-the-shelf hydrogen sensors has shown that no single hydrogen sensing technology can meet all the performance requirements [5]. For example, catalytic combustion-type and resistance-type sensors may cause the catalyst to undergo high-temperature sintering and detachment under high hydrogen concentration, while the detection limit of thermal conductivity type sensors is insufficient. By integrating different sensing technologies into a single detection device, the detection requirements for different concentrations can be met [73]. By combining catalytic combustion sensors with thermal conductivity sensors, it is possible to detect hydrogen concentrations up to 100%, without the need for oxygen. This effectively enhances the safety and reliability of the system. Moreover, to account for the influence of environmental temperature and humidity, temperature and humidity sensing elements can be integrated into the hydrogen detection equipment to compensate for the detection results. Therefore, while optimizing the detection technology, exploring methods to combine different sensing technologies in a single detection device seems to be a feasible approach.

In conclusion, the design requirements for efficient hydrogen sensors involve comprehensive control from the microscopic to the macroscopic levels. Unlike conventional usage scenarios, for vehicle applications, it is more important to address the sensor's accelerated failure due to environmental humidity and vibration. However, there is still a lack of research in this area. As the commercialization of hydrogen fuel cell vehicles accelerates, high-performance, low-cost, and long-life onboard hydrogen sensors will become the focus of the next-generation technological competition.

5. Conclusions

This paper reviews the performance requirements and design concepts of catalytic combustion hydrogen sensors for vehicle applications, providing theoretical guidance for the research and development of vehicle hydrogen sensors. The key to improving the performance of hydrogen sensors lies in two aspects: catalyst development and the integration process. Future improvement directions can be considered from the following points:

- From the perspective of the reaction mechanism of hydrogen oxidation, promoting the supply of oxygen during the reaction is an effective means to improve device performance. It can be improved by designing reducible supports such as CeO_2 and TiO_2 or increasing O_2 adsorption activation sites;
- The development of low-temperature hydrogen oxidation catalysts can effectively reduce the sensor's response to other combustible gases, but the cross-response to CO remains a difficult problem to solve;
- In situ generation of catalytic materials on the substrate will greatly reduce the thermal loss during the operation of the sensor and improve the stability of the sensitive element. Developing catalysts with special morphological structures can further enhance the response rate and sensitivity of the device;
- In the vehicle environment, pollutants such as organosilicon are prone to exist, leading to catalyst poisoning. Catalyst modification and coating of filter layers can alleviate the process of silicon poisoning to a certain extent, but permanent deactivation under long-term poisoning cannot be avoided. Studying the catalyst regeneration mechanism and developing regeneration procedures may be another feasible solution to improve the service life of hydrogen sensors;
- Due to the scaling law, the significant reduction in the size of the micro-heater also correspondingly shortens the thermal response time, thereby achieving low duty cycle

operation and further reducing power consumption. For vehicle sensors, the seismic performance cannot be ignored, but there are few studies in the literature in this regard. Although the reported sensors generally have ideal performance, from the perspective of the convenience of the preparation process and manufacturing cost, it is unfavorable for both large-scale industrial production and simplification of the production process;

- The future development of onboard catalytic combustion hydrogen sensors will focus on breakthroughs in intelligence and self-maintenance systems, such as dynamically compensating for signal drift through artificial intelligence algorithms to achieve high-precision self-calibration; developing multi-gas sensing fusion technology to enhance the anti-interference ability in complex environments; and exploring self-repairing catalytic materials to extend the sensor lifespan to the vehicle's service period. These innovative directions will drive the hydrogen detection process to evolve from a single function to an integrated perception-diagnosis-protection intelligent safety system, ultimately meeting the inherent safety requirements of hydrogen fuel cell vehicles.

Although the catalytic combustion hydrogen sensor technology is mature, its application in vehicles still faces three core challenges: harsh working conditions (vibration/temperature variation/polluting gases) impose higher requirements on reliability, response speed, and anti-interference ability; reliance on precious metals and anti-poisoning packaging processes increase manufacturing costs and the manufacturability urgently needs breakthroughs in substrate innovation; and mechanical vibration stress, silicon oxide poisoning, and high-concentration hydrogen gas impact pose continuous risks for practical implementation. To address these bottlenecks, future breakthroughs need to focus on catalyst modification, regeneration program design, the development of multi-sensor technology integrating catalytic and thermal conductivity modes, and innovation in artificial intelligence algorithms. Only by collaborating on the integration of material design and process integration can we develop vehicle hydrogen sensors that are adaptable to all-weather working conditions and have both rapid and accurate detection and long-term lifespan.

Author Contributions: B.H. wrote the paper; Y.W. and C.W. designed the structure of the paper; L.W. and S.Y. reviewed the paper. All authors have read and agreed to the published version of the manuscript.

Funding: This research was funded by the Science and Technology Program Projects of Zhejiang Provincial Administration for Market Regulation (ZD2024006), Zhejiang Provincial Natural Science Foundation of China (LQN25E060007), and the Science and Technology Program of Taizhou (24gyb54).

Data Availability Statement: Data are contained within the article.

Conflicts of Interest: The authors declare no conflicts of interest.

References

1. Hydrogen Council. *Hydrogen Scaling Up: A Sustainable Pathway for the Global Energy Transition*; Hydrogen Council: Brussels, Belgium, 2017; Available online: https://hydrogencouncil.com/en/study-hydrogen-scaling-up/ (accessed on 11 June 2025).
2. Song, K.; Hou, T.; Jiang, J.; Grigoriev, S.A.; Fan, F.; Qin, J.; Wang, Z.; Sun, C. Thermal management of liquid-cooled proton exchange membrane fuel cell: A review. *J. Power Sources* **2025**, *648*, 237227. [CrossRef]
3. Debe, M.K. Electrocatalyst approaches and challenges for automotive fuel cells. *Nature* **2012**, *486*, 43–51. [CrossRef]
4. Li, F.; Yuan, Y.; Yan, X.; Malekian, R.; Li, Z. A study on a numerical simulation of the leakage and diffusion of hydrogen in a fuel cell ship. *Renew. Sustain. Energy Rev.* **2018**, *97*, 177–185. [CrossRef]
5. Boon-Brett, L.; Bousek, J.; Black, G.; Moretto, P.; Castello, P.; Huebert, T.; Banach, U. Identifying performance gaps in hydrogen safety sensor technology for automotive and stationary applications. *Int. J. Hydrog. Energy* **2010**, *35*, 373–384. [CrossRef]

6. Foorginezhad, S.; Mohseni-Dargah, M.; Falahati, Z.; Abbassi, R.; Razmjou, A.; Asadnia, M. Sensing advancement towards safety assessment of hydrogen fuel cell vehicles. *J. Power Sources* **2021**, *489*, 229450. [CrossRef]
7. Boon-Brett, L.; Bousek, J.; Moretto, P. Reliability of commercially available hydrogen sensors for detection of hydrogen at critical concentrations: Part II—Selected sensor test results. *Int. J. Hydrog. Energy* **2009**, *34*, 562–571. [CrossRef]
8. NISSHA FIS Inc. FH2-HY11 [Product Information]. Available online: https://www.fisinc.co.jp/products/products_search.html?Cat=Cat1 (accessed on 11 June 2025).
9. Niu, G.; Wang, F. A review of MEMS-based metal oxide semiconductors gas sensor in Mainland China. *J. Micromech. Microeng.* **2022**, *32*, 054003. [CrossRef]
10. Ladacki, M.; Houser, T.J.; Roberts, R.W. Catalyzed Low-Temperature Hydrogen-Oxygen Reaction. *J. Catal.* **1965**, *4*, 239–247. [CrossRef]
11. Lee, J.-S.; An, J.W.; Bae, S.; Lee, S.-K. Review of Hydrogen Gas Sensors for Future Hydrogen Mobility Infrastructure. *Appl. Sci. Converg. Technol.* **2022**, *31*, 79–84. [CrossRef]
12. Oigawa, H.; Shimojima, M.; Tsuno, T.; Ueda, T. Stable Heating Technology for Catalytic Combustion Hydrogen Gas Sensor Using Quartz Resonators. *Sens. Mater.* **2018**, *30*, 1103–1114.
13. Henriquez, D.D.O.; Cho, I.; Yang, H.; Choi, J.; Kang, M.; Chang, K.S.; Jeong, C.B.; Han, S.W.; Park, I. Pt Nanostructures Fabricated by Local Hydrothermal Synthesis for Low-Power Catalytic-Combustion Hydrogen Sensors. *ACS Appl. Nano Mater.* **2021**, *4*, 7–12. [CrossRef]
14. Kalinin, I.A.; Roslyakov, I.V.; Bograchev, D.; Kushnir, S.E.; Ivanov, I.I.; Dyakov, A.V.; Napolskii, K.S. High performance microheater-based catalytic hydrogen sensors fabricated on porous anodic alumina substrates. *Sens. Actuators B* **2024**, *404*, 135270. [CrossRef]
15. Lee, E.-B.; Hwang, I.-S.; Cha, J.-H.; Lee, H.-J.; Lee, W.-B.; Pak, J.J.; Lee, J.-H.; Ju, B.-K. Micromachined catalytic combustible hydrogen gas sensor. *Sens. Actuators B* **2011**, *153*, 392–397. [CrossRef]
16. Wettergren, K.; Hellman, A.; Cavalca, F.; Zhdanov, V.P.; Langhammer, C. Unravelling the Dependence of Hydrogen Oxidation Kinetics on the Size of Pt Nanoparticles by in Operando Nanoplasmonic Temperature Sensing. *Nano Lett.* **2015**, *15*, 574–580. [CrossRef]
17. Fassihi, M.; Zhdanov, V.P.; Rinnemo, M.; Keck, K.E.; Kasemo, B. A Theoretical and Experimental-Study of Catalytic Ignition in the Hydrogen Oxygen Reaction on Platinum. *J. Catal.* **1993**, *141*, 438–452. [CrossRef]
18. Schwarzer, M.; Borodin, D.; Wang, Y.; Fingerhut, J.; Kitsopoulos, T.N.; Auerbach, D.J.; Guo, H.; Wodtke, A.M. Cooperative adsorbate binding catalyzes high-temperature hydrogen oxidation on palladium. *Science* **2024**, *386*, 511–516. [CrossRef]
19. Liu, Y.; Koo, K.; Mao, Z.; Fu, X.; Hu, X.; Dravid, V.P. Unraveling the adsorption- limited hydrogen oxidation reaction at palladium surface via in situ electron microscopy. *Proc. Natl. Acad. Sci. USA* **2024**, *121*, e2408277121. [CrossRef]
20. Singh, S.A.; Vishwanath, K.; Madras, G. Role of Hydrogen and Oxygen Activation over Pt and Pd-Doped Composites for Catalytic Hydrogen Combustion. *ACS Appl. Mater. Interfaces* **2017**, *9*, 19380–19388. [CrossRef]
21. Kim, J.; Tahmasebi, A.; Lee, J.M.; Lee, S.; Jeon, C.-H.; Yu, J. Low-temperature catalytic hydrogen combustion over Pd-Cu/Al_2O_3: Catalyst optimization and rate law determination. *Korean J. Chem. Eng.* **2023**, *40*, 1317–1330. [CrossRef]
22. Owais, T.; Khater, M.; Al-Qahtani, H. Graphene-based MEMS devices for gas sensing applications: A review. *Micro Nanostruct.* **2024**, *195*, 207954. [CrossRef]
23. Pan, Y.; Xu, H.; Chen, M.; Wu, K.; Zhang, Y.; Long, D. Unveiling the Nature of Room-Temperature O_2 Activation and $O_2^{\bullet}$-Enrichment on MgO-Loaded Porous Carbons with Efficient H_2S Oxidation. *ACS Catal.* **2021**, *11*, 5974–5983. [CrossRef]
24. Zhao, L.; Luo, W.; Huang, Z.; Yan, Z.; Jia, H.; Pei, W.; Tu, Y. Oxygen dissociation on the C3N monolayer: A first-principles study. *Appl. Surf. Sci.* **2023**, *613*, 155912. [CrossRef]
25. Wu, J.; Li, Z.; Xie, X.; Tao, K.; Liu, C.; Khor, K.A.; Miao, J.; Norford, L.K. 3D superhydrophobic reduced graphene oxide for activated NO_2 sensing with enhanced immunity to humidity. *J. Mater. Chem. A* **2018**, *6*, 478–488. [CrossRef]
26. Harley-Trochimczyk, A.; Chang, J.; Zhou, Q.; Dong, J.; Pham, T.; Worsley, M.A.; Maboudian, R.; Zettl, A.; Mickelson, W. Catalytic hydrogen sensing using microheated platinum nanoparticle-loaded graphene aerogel. *Sens. Actuators B* **2015**, *206*, 399–406. [CrossRef]
27. Aasmundtveit, K.E.; Roy, A.; Ta, B.Q. Direct Integration of Carbon Nanotubes in CMOS, Towards an Industrially Feasible Process: A Review. *IEEE Trans. Nanotechnol.* **2020**, *19*, 113–122. [CrossRef]
28. Chen, M.; Zhang, H.; Li, H.; Zhao, Z.; Wang, K.; Zhou, Y.; Zhao, X.; Dubal, D.P. CxNy-based materials as gas sensors: Structure, performance, mechanism and perspective. *Coord. Chem. Rev.* **2024**, *503*, 215653. [CrossRef]
29. Wang, Z.; Zhang, B.; Yang, S.; Yang, X.; Meng, F.; Zhai, L.; Li, Z.; Zhao, S.; Zhang, G.; Qin, Y. Dual Pd2+and Pd0 sites on CeO2 for benzyl alcohol selective oxidation. *J. Catal.* **2022**, *414*, 385–393. [CrossRef]
30. Deshpande, P.A.; Madras, G. Catalytic hydrogen combustion for treatment of combustible gases from fuel cell processors. *Appl. Catal. B* **2010**, *100*, 481–490. [CrossRef]
31. Kim, J.; Yu, J.; Lee, S.; Tahmasebi, A.; Jeon, C.-H.; Lucas, J. Advances in catalytic hydrogen combustion research: Catalysts, mechanism, kinetics, and reactor designs. *Int. J. Hydrog. Energy* **2021**, *46*, 40073–40104. [CrossRef]

32. Yu, J.; Yang, Y.; Zhang, M.; Song, B.; Han, Y.; Wang, S.; Ren, Z.; Wang, L.; Yin, P.; Zheng, L.; et al. Highly Active $MnCoO_x$ Catalyst toward CO Preferential Oxidation. *ACS Catal.* **2024**, *14*, 1281–1291. [CrossRef]
33. Han, C.-H.; Hong, D.-W.; Kim, I.-J.; Gwak, J.; Han, S.-D.; Singh, K.C. Synthesis of Pd or Pt/titanate nanotube and its application to catalytic type hydrogen gas sensor. *Sens. Actuators B* **2007**, *128*, 320–325. [CrossRef]
34. Wang, Y.; Zhao, Z.; Sun, Y.; Li, P.; Ji, J.; Chen, Y.; Zhang, W.; Hu, J. Fabrication and gas sensing properties of Au-loaded SnO_2 composite nanoparticles for highly sensitive hydrogen detection. *Sens. Actuators B* **2017**, *240*, 664–673. [CrossRef]
35. Brauns, E.; Morsbach, E.; Kunz, S.; Baeumer, M.; Lang, W. A fast and sensitive catalytic gas sensors for hydrogen detection based on stabilized nanoparticles as catalytic layer. *Sens. Actuators B* **2014**, *193*, 895–903. [CrossRef]
36. Heinz, H.; Pramanik, C.; Heinz, O.; Ding, Y.; Mishra, R.K.; Marchon, D.; Flatt, R.J.; Estrela-Lopis, I.; Llop, J.; Moya, S.; et al. Nanoparticle decoration with surfactants: Molecular intercations, assmbly, and applications. *Surf. Sci. Rep.* **2017**, *72*, 1–58. [CrossRef]
37. Balandin, A.A.; Ghosh, S.; Bao, W.; Calizo, I.; Teweldebrhan, D.; Miao, F.; Lau, C.N. Superior thermal conductivity of single-layer graphene. *Nano Lett.* **2008**, *8*, 902–907. [CrossRef]
38. Nan, H.Y.; Ni, Z.H.; Wang, J.; Zafar, Z.; Shi, Z.X.; Wang, Y.Y. The thermal stability of graphene in air investigated by Raman spectroscopy. *J. Raman Spectrosc.* **2013**, *44*, 1018–1021. [CrossRef]
39. Yazawa, Y.; Yoshida, H.; Komai, S.; Hattori, T. The additive effect on propane combustion over platinum catalyst: Control of the oxidation-resistance of platinum by the electronegativity of additives. *Appl. Catal. A* **2002**, *233*, 113–124. [CrossRef]
40. Del Orbe, D.V.; Yang, H.; Cho, I.; Park, J.; Choi, J.; Han, S.W.; Park, I. Low-power thermocatalytic hydrogen sensor based on electrodeposited cauliflower-like nanostructured Pt black. *Sens. Actuators B* **2021**, *329*, 129129. [CrossRef]
41. Rao, A.; Long, H.; Harley-Trochimczyk, A.; Thang, P.; Zettl, A.; Carraro, C.; Mahoudian, R. In Situ Localized Growth of Ordered Metal Oxide Hollow Sphere Array on Microheater Platform for Sensitive, Ultra-Fast Gas Sensing. *ACS Appl. Mater. Interfaces* **2017**, *9*, 2634–2641. [CrossRef]
42. Wang, P.; Tian, X.; Yan, M.; Yang, B.; Hua, Z. A low temperature catalytic-type combustible gas sensor based on Pt supported zeolite catalyst films. *J. Mater. Sci.* **2021**, *56*, 4666–4676. [CrossRef]
43. Liu, X.; Dong, H.; Xia, S. Micromachined Catalytic Combustible Hydrogen Gas Sensor Based on Nano-structured SnO_2. *Acta Chim. Sinica* **2013**, *71*, 657–662. [CrossRef]
44. Baranov, A.; Ivanov, I.; Karpova, E. Effects of Flameless Catalytic Combustion of Hydrogen on the Parameters of Catalytic Sensors with Platinum-group Catalysts. *Sens. Mater.* **2023**, *35*, 3585–3594. [CrossRef]
45. Ivanov, I.; Baranov, A.; Mironov, S.; Talipov, V.; Karami, H.; Gharehpetian, G.B. Development of an Approach to Increase Hydrogen Measurement Selectivity. *Sens. Mater.* **2023**, *35*, 1045. [CrossRef]
46. Chen, W.; Cao, J.; Fu, W.; Zhang, J.; Qian, G.; Yang, J.; Chen, D.; Zhou, X.; Yuan, W.; Duan, X. Molecular-Level Insights into the Notorious CO Poisoning of Platinum Catalyst. *Angew. Chem. Int. Ed.* **2022**, *61*, e202200190. [CrossRef]
47. Bao, S.; Yang, L.; Fu, H.; Qu, X.; Zheng, S. Fine Ru-Ru_2P Heterostructure Enables Highly Active and Selective CO_2 Hydrogenation to CO. *ACS Catal.* **2024**, *14*, 18134–18144. [CrossRef]
48. Yue, L.; Zhao, W.; Li, J.; Wu, R.; Wang, Y.; Zhang, H.; Zhao, Y. Low-temperature CO preferential oxidation in H_2-rich stream over Indium modified Pd-Cu/Al_2O_3 catalyst. *J. Colloid Interface Sci.* **2024**, *662*, 109–118. [CrossRef]
49. Zhao, W.; Yue, L.; Li, J.; Kong, L.; Chen, Z.; Zheng, K.; Zhang, L.; Wang, C.; Wu, R.; Wang, Y.; et al. Pd species aggregation state regulation of Pd-Cu/Al_2O_3 for low-temperature CO preferential oxidation. *Chem. Eng. J.* **2025**, *518*, 164668. [CrossRef]
50. Liu, S.; Gong, S.; Feng, H.; Ma, Z.; Yang, L.; Li, P. Selective hydrogen combustion in the presence of propylene and propane over Pt/A-zeolite catalysts. *Int. J. Hydrog. Energy* **2020**, *45*, 12347–12359. [CrossRef]
51. Matsumiya, M.; Shin, W.S.; Qiu, F.B.; Izu, N.; Matsubara, I.; Murayama, N. Poisoning of platinum thin film catalyst by hexamethyldisiloxane (HMDS) for thermoelectric hydrogen gas sensor. *Sens. Actuators B* **2003**, *96*, 516–522. [CrossRef]
52. Gentry, S.J.; Jones, A. Poisoning and inhibition of catalytic oxidations: 1. Effect of silicone vapor on the gas-phase oxidations of methane, propene, carbon-monoxide and hydrogen over platinum and palladium catalysts. *J. Appl. Chem. Biotechnol.* **1978**, *28*, 727–732. [CrossRef]
53. Rahmani, M.; Sohrabi, M. Si-tolerance of iron doped Pt/alumina catalyst in the total oxidation of VOC. *React. Kinet. Catal. Lett.* **2005**, *86*, 397–405. [CrossRef]
54. Porras, S.; Sippula, O.; Mesceriakove, S.-M.; Maunula, T.; Kallinen, K.; Suvanto, M.; Kinnunen, N.M. Poisoning of automotive methane oxidation catalysts by silicon compounds. *Chem. Eng. Sci.* **2023**, *282*, 119268. [CrossRef]
55. Xu, H.; Li, J.; Fu, Y.; Luo, W.; Tian, Y. Deactivation mechanism and anti-deactivation modification of SnO_2-based catalysts for methane gas sensors. *Sens. Actuators B* **2019**, *299*, 126939. [CrossRef]
56. Chao, Y.T.; Yao, S.; Buttner, W.J.; Stetter, J.R. Amperometric sensor for selective and stable hydrogen measurement. *Sens. Actuators B* **2005**, *106*, 784–790.
57. Kwon, Y.M.; Kim, H.-J.; Ye, B.; Kim, H.-D.; Lee, Y.S.; Shin, H.; Baik, J.M. Ce oxide nanoparticles on porous reduced graphene oxides for stable hydrogen detection in air/HMDSO environment. *Sens. Actuators B* **2020**, *321*, 128529. [CrossRef]

58. Moon, Y.K.; Jeong, S.-Y.; Kang, Y.C.; Lee, J.-H. Metal Oxide Gas Sensors with Au Nanocluster Catalytic Overlayer: Toward Tuning Gas Selectivity and Response Using a Novel Bilayer Sensor Design. *ACS Appl. Mater. Interfaces* **2019**, *11*, 32169–32177. [CrossRef]
59. Liu, W.; Zou, J.; Li, S.; Li, J.; Li, F.; Zhan, Z.; Zhang, Y. Pd/In_2O_3-based bilayer H_2 sensor with high resistance to silicone toxicity and ultra-fast response. *Int. J. Hydrogen Energy* **2023**, *48*, 5743–5753. [CrossRef]
60. Ehrhardt, J.J.; Colin, L.; Jamois, D. Poisoning of platinum surfaces by hexamethyldisiloxane (HMDS): Application to catalytic methane sensors. *Sens. Actuators B* **1997**, *40*, 117–124. [CrossRef]
61. Arnby, K.; Rahmani, M.; Sanati, M.; Cruise, N.; Carlsson, A.A.; Skoglundh, M. Characterization of Pt/-γ-Al_2O_3 catalysts deactivated by hexamethyldisiloxane. *Appl. Catal. B* **2004**, *54*, 1–7. [CrossRef]
62. Rasmussen, S.B.; Kustov, A.; Skotte, J.; Siret, B.; Tabaries, F.; Fehrmann, R. Characterization and regeneration of Pt-catalysts deactivated in municipal waste flue gas. *Appl. Catal. B* **2006**, *69*, 10–16. [CrossRef]
63. Fernandez, A.; Arzac, G.M.; Vogt, U.F.; Hosoglu, F.; Borgschulte, A.; Jimenez de Haro, M.C.; Montes, O.; Zuettel, A. Investigation of a Pt containing washcoat on SiC foam for hydrogen combustion applications. *Appl. Catal. B* **2016**, *180*, 336–343. [CrossRef]
64. Li, H.; Wu, R.; Liu, H.-B.; Han, L.-Y.; Yuan, W.-J.; Hua, Z.-Q.; Fan, S.-R.; Wu, Y. A novel catalytic-type gas sensor based on alumina ceramic substrates loaded with catalysts and printed electrodes. *Chin. J. Anal. Chem.* **2021**, *49*, 93–101. [CrossRef]
65. Xu, D.; Xu, P.; Wang, X.; Chen, Y.; Yu, H.; Zheng, D.; Li, X. Pentagram-Shaped Ag@Pt Core-Shell Nanostructures as High-Performance Catalysts for Formaldehyde Detection. *ACS Appl. Mater. Interfaces* **2020**, *12*, 8091–8097. [CrossRef]
66. Choi, K.-W.; Lee, J.-S.; Seo, M.-H.; Jo, M.-S.; Yoo, J.-Y.; Sim, G.S.; Yoon, J.-B. Batch-fabricated CO gas sensor in large-area (8-inch) with sub-10 mW power operation. *Sens. Actuators B* **2019**, *289*, 153–159. [CrossRef]
67. Chen, Y.; Xu, P.; Li, X.; Ren, Y.; Deng, Y. High-performance H_2 sensors with selectively hydrophobic micro-plate for self-aligned upload of Pd nanodots modified mesoporous In_2O_3 sensing-material. *Sens. Actuators B* **2018**, *267*, 83–92. [CrossRef]
68. Jo, M.-S.; Kim, K.-H.; Lee, J.-S.; Kim, S.-H.; Yoo, J.-Y.; Choi, K.-W.; Kim, B.-J.; Kwon, D.-S.; Yoo, I.; Yang, J.-S.; et al. Ultrafast (∼0.6 s), Robust, and Highly Linear Hydrogen Detection up to 10% Using Fully Suspended Pure Pd Nanowire. *ACS Nano* **2023**, *17*, 23649–23658. [CrossRef]
69. Watanabe, M.; Inoue, R.; Ichikawa, D.; Furusaki, K. Development of Thermal Conductivity Type Hydrogen Sensor. In Proceedings of the Symposium on Sensors, Actuators, and Microsystems General Session Held During the 217th Meeting of the Electrochemical-Society (ECS), Vancouver, BC, Canada, 25–30 April 2010; pp. 31–42.
70. Chang, H.S.; Son, G.G.; Park, J.Y.; Hyung, S.J.; Park, J.S. Development and Application of Hydrogen Sensor Evaluation Rig for FCEV. *Int. J. Automot. Technol.* **2025**. [CrossRef]
71. Xie, B.; Liu, Y.; Lei, Y.; Qian, H.; Li, Y.; Yan, W.; Zhou, C.; Wen, H.-M.; Xia, S.; Mao, P.; et al. Innovative Thermocatalytic H_2 Sensor with Double-Sided Pd Nanocluster Films on an Ultrathin Mica Substrate. *ACS Sens.* **2024**, *9*, 2529–2539. [CrossRef]
72. Girma, H.G.; Park, K.H.; Ji, D.; Kim, Y.; Lee, H.M.; Jeon, S.; Jung, S.-H.; Kim, J.Y.; Noh, Y.-Y.; Lim, B. Room-Temperature Hydrogen Sensor with High Sensitivity and Selectivity using Chemically Immobilized Monolayer Single-Walled Carbon Nanotubes. *Adv. Funct. Mater.* **2023**, *33*, 2213381. [CrossRef]
73. Huebert, T.; Boon-Brett, L.; Palmisano, V.; Bader, M.A. Developments in gas sensor technology for hydrogen safety. *Int. J. Hydrog. Energy* **2014**, *39*, 20474–20483. [CrossRef]
74. Kondalkar, V.V.; Park, J.; Lee, K. MEMS hydrogen gas sensor for in-situ monitoring of hydrogen gas in transformer oil. *Sens. Actuators B* **2021**, *326*, 128989. [CrossRef]
75. Saxena, G.; Paily, R. Analytical Modeling of Square Microhotplate for Gas Sensing Application. *IEEE Sens. J.* **2013**, *13*, 4851–4859. [CrossRef]
76. Liu, Q.; Yao, J.; Wu, Y.; Wang, Y.; Ding, G. Two operating modes of palladium film hydrogen sensor based on suspended micro hotplate. *Int. J. Hydrog. Energy* **2019**, *44*, 11259–11265. [CrossRef]
77. Samaeifar, F.; Afifi, A.; Abdollahi, H. Simple Fabrication and Characterization of a Platinum Microhotplate Based on Suspended Membrane Structure. *Exp. Tech.* **2016**, *40*, 755–763. [CrossRef]
78. Spannhake, J.; Schulz, O.; Helwig, A.; Krenkow, A.; Muller, G.; Doll, T. High-temperature MEMS heater platforms:: Long-term performance of metal and semiconductor heater materials. *Sensors* **2006**, *6*, 405–419. [CrossRef]
79. Coppola, G.; Striano, V.; Ferraro, P.; De Nicola, S.; Finizio, A.; Pierattini, G.; Maccagnani, P. A nondestructive dynamic characterization of a microheater through digital holographic microscopy. *J. Microelectromech. Syst.* **2007**, *16*, 659–667. [CrossRef]
80. Behera, B.; Chandra, S. An innovative gas sensor incorporating ZnO-CuO nanoflakes in planar MEMS technology. *Sens. Actuators B* **2016**, *229*, 414–424. [CrossRef]
81. Urasinska-Wojcik, B.; Vincent, T.A.; Chowdhury, M.F.; Gardner, J.W. Ultrasensitive WO_3 gas sensors for NO_2 detection in air and low oxygen environment. *Sens. Actuators B* **2017**, *239*, 1051–1059. [CrossRef]
82. Xie, D.; Liu, R.; Adedokun, G.; Xu, L.; Wu, F. A Novel Low Power Hexagonal Gas Sensor Cell for Multi-Channel Gas Detection. In Proceedings of the 34th IEEE International Conference on Micro Electro Mechanical Systems (MEMS), Electr Network, Virtual, 25–29 January 2021; pp. 430–433.

83. Liu, Q.; Ding, G.; Wang, Y.; Yao, J. Thermal Performance of Micro Hotplates with Novel Shapes Based on Single-Layer SiO_2 Suspended Film. *Micromachines* **2018**, *9*, 514. [CrossRef]
84. Coppeta, R.; Lahlalia, A.; Kozic, D.; Hammer, R.; Riedler, J.; Toschkoff, G.; Singulani, A.; Ali, Z.; Sagmeister, M.; Carniello, S.; et al. Electro-Thermal-Mechanical Modeling of Gas Sensor Hotplates. In *Sensor Systems Simulations: From Concept to Solution*; van Driel, W.D., Pyper, O., Schumann, C., Eds.; Springer International Publishing: Cham, Switzerland, 2020; pp. 17–72.

Disclaimer/Publisher's Note: The statements, opinions and data contained in all publications are solely those of the individual author(s) and contributor(s) and not of MDPI and/or the editor(s). MDPI and/or the editor(s) disclaim responsibility for any injury to people or property resulting from any ideas, methods, instructions or products referred to in the content.